Science of the Total Environment 907 (2024) 168026

Contents lists available at ScienceDirect

Science of the Total Environment

journal homepage: www.elsevier.com/locate/scitotenv

Ecological strategies of bacterial communities in prehistoric stone wall paintings across weathering gradients: A case study from the Borana zone in southern Ethiopia

Gianmarco Mugnai [a], Luigimaria Borruso [b,1], Ying-Li Wu [c,2], Marina Gallinaro [d], Francesca Cappitelli [e], Andrea Zerboni [c], Federica Villa [e,*]

[a] Department of Agriculture, Food and Environmental Sciences, University of Perugia, Borgo XX Giugno, 74, I-06121 Perugia (PG), IT, Italy
[b] Free University of Bolzano, Faculty of Agricultural, Environmental and Food Sciences, Piazza Universitá 5, 39100 Bolzano, Italy
[c] Dipartimento di Scienze della Terra "A. Desio", Università degli Studi di Milano, 20133 Milan, Italy
[d] Dipartimento di Scienze dell'Antichità, Università di Roma La Sapienza, 00185 Rome, Italy
[e] Dipartimento di Scienze per gli Alimenti, la Nutrizione e l'Ambiente, Università degli Studi di Milano, 20133 Milan, Italy

HIGHLIGHTS

- Lowly- and highly-weathered samples harbor k-strategist microorganisms and reduced α-diversity.
- Lowly- and highly-weathered samples host bacteria with a positive or neutral impact on the stone.
- Moderately-weathered samples exhibit diverse microhabitats, selecting for r-strategist bacteria.
- Moderately-weathered surfaces show increased α-diversity and specialist microorganisms.
- Bacteria in moderately-weathered samples negatively impact the stone.

GRAPHICAL ABSTRACT

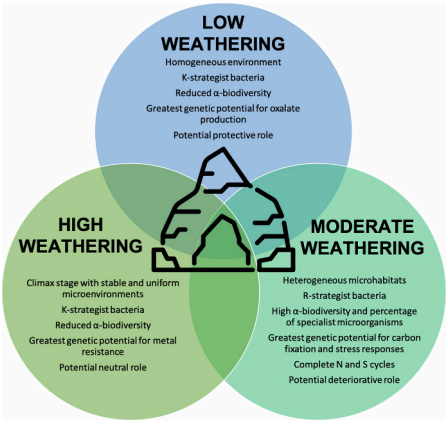

ARTICLE INFO

Guest Editor: Patricia Sanmartin

Keywords:
Bacterial community
Predicted metagenomes
Rock art paintings

ABSTRACT

Rock art paintings represent fragile ecosystems supporting complex microbial communities tuned to the lithic substrate and climatic conditions. The composition and activity of these microbial communities associated with different weathering patterns affecting rock art sites remain unexplored. This study aimed to explore how bacterial communities adapt their ecological strategies based on substrate weathering, while also examining the role of their metabolic pathways in either biodeterioration or bioprotection of the underlying stone. SEM-EDS

* Corresponding author.
E-mail addresses: gianmarco.mugnai@unipg.it (G. Mugnai), luigimaria.borruso@unibz.it (L. Borruso), ying.wu@unimi.it, ying-li.wu@uwa.edu.au (Y.-L. Wu), marina.gallinaro@uniroma1.it (M. Gallinaro), francesca.cappitelli@unimi.it (F. Cappitelli), andrea.zerboni@unimi.it (A. Zerboni), federica.villa@unimi.it (F. Villa).
[1] Co-first author.
[2] Current affiliation: School of Social Sciences, Centre for Rock Art Research and Management M257, 35 Stirling Hwy, Perth WA 6009, Australia.

https://doi.org/10.1016/j.scitotenv.2023.168026
Received 10 August 2023; Received in revised form 18 September 2023; Accepted 20 October 2023
Available online 29 October 2023

Stone weathering degrees
Ecological strategies

investigations coupled with 16S rRNA gene sequencing and PICRUSt2 analysis were applied on different weathered surfaces that affect southern Ethiopian rock paintings to investigate the relationships between the current stone microbiome and weathering patterns. The findings revealed that samples experiencing low and high weathering reached a climax stage characterized by stable microenvironments and limited resources. This condition favored K-strategist microorganisms, leading to reduced α-biodiversity and a community with a positive or neutral impact on the substrate. In contrast, moderately-weathered samples displayed diverse microhabitats, resulting in the prevalence of r-strategist bacteria, increased α-biodiversity, and the presence of specialist microorganisms. Moreover, the bacterial communities in moderately-weathered samples demonstrated the highest potential for carbon fixation, stress responses, and complete nitrogen and sulfur cycles. This bacterial community also showed the potential to negatively impact the underlying substrate. This research provided valuable insights into the little-understood ecology of bacterial communities inhabiting deteriorated surfaces, shedding light on the potential role of these microorganisms in the sustainable conservation of rock art.

1. Introduction

Rock art, which encompasses various forms of painting and engraving on natural rock surfaces, is a practice that predates recorded history by many millennia. It is a powerful testimony to the creativity and agency of our ancestors and represents a significant archive of their past (Gallinaro et al., 2018). However, given its age and vulnerability to the unpredictable and ever-changing conditions of nature, rock art requires careful preservation and protection measures to ensure its survival for future generations.

Despite being considered a harsh environment, the lithic surfaces that host paintings and engravings can be colonized by subaerial biofilms (SABs), complex communities of microorganisms at the mineral-air interface that are embedded in a self-produced extracellular polymeric matrix (Villa and Cappitelli, 2019; Zerboni et al., 2022). SABs are finely tuned ecosystems that interact with and adapt to their specific substrate and external environment (Villa et al., 2016). As a result, they play a critical role in the micro-scale processes that occur on lithic surfaces, both in terms of preservation and deterioration of rock art. For many years SABs have been identified as key players in stone monuments deterioration. Their presence has been linked to various detrimental effects, including physical and chemical changes, e.g., encrustation, corrosion induced by biogenic acids, complexation and release of cations, secondary mineralization and (re)crystallization, as well as internal stress and delamination (Liu et al., 2020). So far, the identification of even a single one of these mechanisms on a deteriorated surface is sufficient to attribute the biodeteriogenic effect to the biofilm. However, SABs can also provide bioprotection. This represents the other side of the coin, where biofilms offer physical protection through the formation of a patina or the biomineralization of minerals, as well as chemical benefits as the precipitation and crystallization of salts within the stone matrices (Liu et al., 2022). Thus, SABs exhibit a dual nature, both potentially contributing to deterioration processes and offering protective qualities that help mitigate the impact of environmental stresses on stone surfaces (Favero-Longo and Viles, 2020; Pinna, 2014; Zerboni et al., 2022).

Therefore, the overall impact of a SAB on a lithic surface should be regarded as the interplay between diverse biological processes taking place on the underlying substrate. These processes can either amplify or mitigate the potentially detrimental effects of the SAB, thereby determining its net impact on the stone. A detailed understanding of the metabolic processes of SABs is essential to the study of rock art, as it can shed light on both the preservation and deterioration of these unique cultural artifacts.

Despite the substantial research and published work available on the chemical and physical state of rock art sites worldwide (Andreae et al., 2020; Cañaveras et al., 2022; Huntley et al., 2021; Macholdt et al., 2019), there is still a notable lack of investigations focusing on how microbial community influences the underlying stone or vice versa. Over the past two decades, research on SABs that inhabit rock art has primarily focused on analyzing the structure of the microbial community (Gonzalez et al., 1999; Nir et al., 2019a, b; Portillo et al., 2009; Roldán et al., 2018; Schabereiter-Gurtner et al., 2004; Wu et al., 2020). Up to now, only a limited number of studies have investigated the role of SABs in the deterioration or protection of rock art. Recently, researchers have characterized the microbiome of black coatings associated with petroglyphs from the Negev Desert and the underlying stone to explore potential mineral-microbial interactions (Nir et al., 2022; Rabbachin et al., 2022). The results strongly indicate the predominance of microorganisms belonging to the Bacteria domain (96 %) within the SAB communities, followed by Archea (3 %) and Eukarya (1 %). Their involvement was attributed to several processes, including the leaching of the calcareous matrix from the underlying bedrock, interactions with silicon grains present in the limestone, and the disintegration of the black coating through the mobilization of metal cations (Nir et al., 2022; Rabbachin et al., 2022). However, to the best of our knowledge, no previous study has characterized the microbial communities on rock art across weathering gradients and assessed the combined effect of their metabolic activities on the lithic substrate.

The hypothesis that drove this study posited that various lithic niches, formed by differing degrees of stone weathering, harbored distinct microbial communities that exerted unique influences on the underlying substrate. Thus, this study had a twofold goal: i) to gain new insights into the ecological strategies adopted by the bacterial communities based on the degree of stone weathering observed in rock paintings; ii) to understand how the overall predicted metabolic pathways of the bacterial communities contribute to either the biodeterioration or bioprotection of the underlying substrate. To achieve our research goal, we collected stone samples from two distinct rock art sites in southern Ethiopia that exhibited different patterns of weathering (Gallinaro and Zerboni, 2021a). Both sites showcase bedrock outcrops characterized by a diverse array of surface weathering and coatings, encompassing a comprehensive spectrum of processes that impact the surfaces of rocks. These processes include the disaggregation and exfoliation of rock surfaces, the formation of neoformed minerals, and the occurrence of whitish efflorescence. The coexistence of such a diverse range of phenomena on the same bedrock, subjected to identical climatic conditions, provided us with a unique opportunity to compare the taxonomic and functional trends of the associated bacterial communities. In this context, the type and intensity of weathering processes on the substrate emerged as the primary (macro)variable influencing the bacterial community ecology.

Here, we employed a synergistic approach, combining scanning electron microscopy with energy dispersive spectroscopy (SEM-EDS) to comprehensively characterize the weathered stone samples, while also utilizing high-throughput 16S rRNA gene sequencing to analyze the bacterial community and predict their metabolic pathways. Our study was primarily centered around three key objectives:

i) Clustering rock art samples based on the level of weathered surfaces, aiming to identify different lithic niches that can influence the structure and function of the associated bacterial communities.

ii) Investigating variations in taxonomical groups along different weathered surfaces, providing insights into the selection of specific taxa in response to the diverse substrate conditions.
iii) Predicting the metabolic pathways involved in energy flow (carbon fixation), biogeochemical cycles (nitrogen, sulfur, and phosphorus), stress resistance, and various minerals-cell interactions (such as metal uptake/regulation, calcite precipitation, and oxalate degradation). Through these predictions, we not only identified bacterial ecological strategies associated with specific levels of stone weathering but also, assessed the collective impact of the bacterial community on the underlying substrate.

Our work offers valuable insights into the poorly understood ecology of bacterial communities inhabiting deteriorated surfaces, shedding light on the potential impacts of SABs on the sustainable conservation of rock art.

2. Materials and methods

2.1. Site description and sampling

The open-air rock art shelters under consideration are in the Yabelo woreda of southern Ethiopia, which is part of the Borana Zone within the Oromia Region. The area is situated approximately 600 km south of Addis Ababa. The region has a semi-arid climate with a bi-modal rainfall pattern and experiences an average annual rainfall range of 400–700 mm. The mean annual temperature of the area is around 19 °C, with minimum temperatures of approximately 9 °C and maximum temperatures of around 27 °C. The region's altitude ranges from 450 to 2500 m asl, resulting in a high seasonal variability (Coppock, 1994; Sutter, n.d.). The local geological bedrock primarily comprises granite intrusions and granitic gneiss from the Adola Belt formations, as described by (Clark, 1945). The landscape in the area has been shaped by intense tropical weathering, resulting in a distinct alternation of inselbergs, piles of boulders, tors, and large isolated boulders of granite/metagranite. Additionally, solutional weathering has played a crucial role in the creation of numerous rock shelters along rocky slopes.

One of the shelters here considered, situated in close proximity to the town of Yabelo and named Dhaka Kura (Crow's Rock, therefore referred to as Yabelo site Yab-6 (here labeled as Y) is part of a group of rock shelters developed into granitic rocks and is still actively used by local herders for animal grazing (Fig. 1A-C). The rock paintings in this shelter depict an assortment of geometric shapes and a range of domestic and wild animals on the stone walls. South of Yabelo, the Borema site Bor-1 (here labeled as B) is another rock shelter that features prehistoric paintings on low-grade metamorphic rock (Fig. 1A-B,D). These paintings depict a variety of subjects including camels, anthropomorphic figures, and wild fauna in black and white. Unfortunately, this site has suffered severe damage from modern graffiti made of charcoal and chalk that has covered some of the original paintings. The preservation of these prehistoric paintings is a cause for concern as they are gradually becoming less visible due to the loss of pigments and exfoliation of the rock substrate, while the formation of crusts is also hindering their visibility.

A crucial task in rock art research is to select a sampling protocol that minimizes the risk of damaging the paintings and engravings. We addressed this challenge by collecting small samples from rock surfaces displaying the same types of alteration or damage as seen on the paintings. These samples were taken from the edge of the panels, well

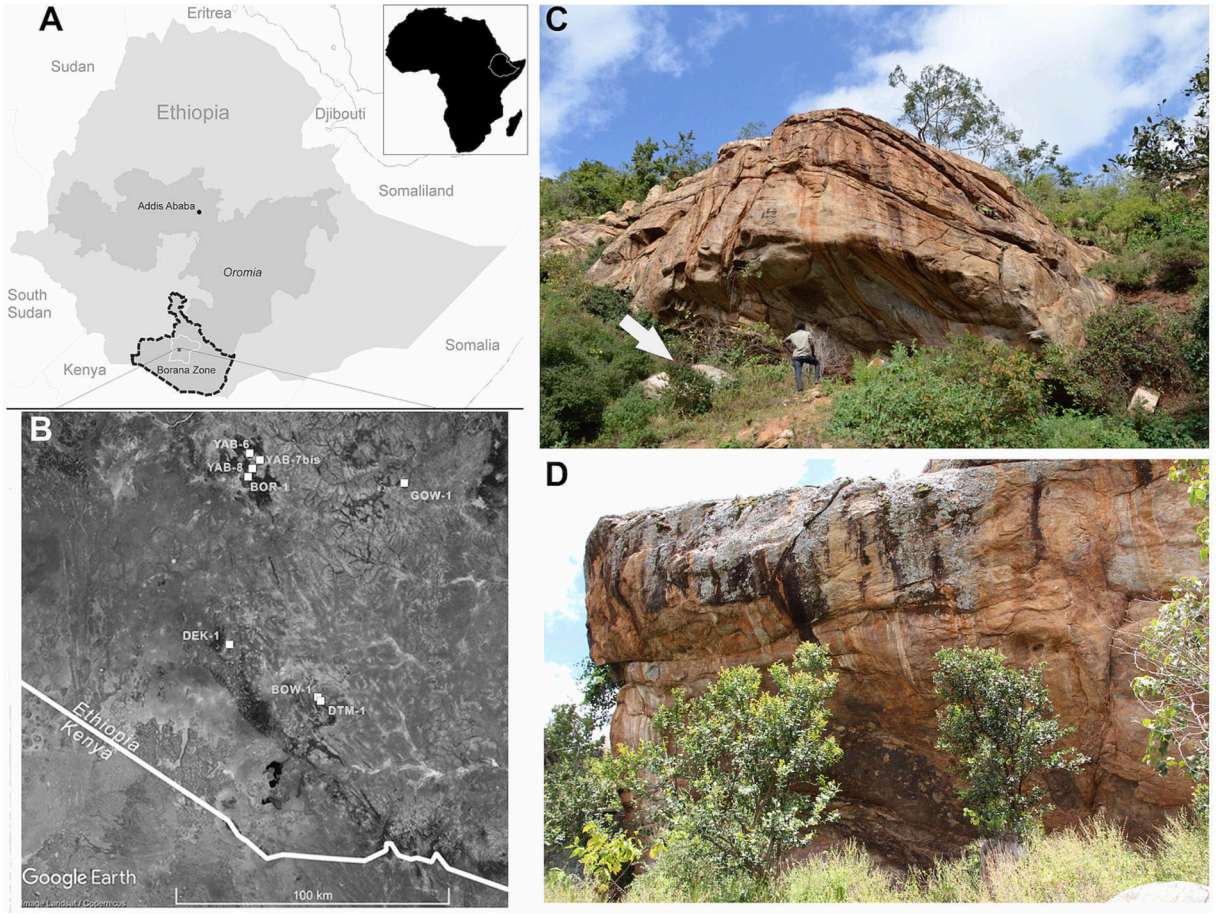

Fig. 1. (A) Position of the study region in Ethiopia and (B) location of the main rock art sites of the area, including Yab-6 (Y-samples) and Bor-1 (B-samples). (C) Yab-6 rock shelter; the arrow indicates the position of sample Y1. (D) General view of the Bor-1 rock shelter.

away from the actual artwork. To collect the samples, we used a sterile scalpel or small chisel and placed them into sterile containers to preserve their integrity. Then, the samples were subdivided into smaller subsamples: one for the molecular investigation and the other for the mineralogical analyses. For molecular analyses, the samples were stored in DNA/RNA Shield (Zymo Research) solution to preserve genetic material at ambient temperature. In total, we selected four samples from the Yabelo site and three from the Borema site. The selection was based on careful observation of the type and rate of rock decay at each site, and aimed at providing a broad characterization of the weathering processes affecting the rocks. By using this approach, we obtained representative samples that provided valuable insights into the nature and extent of rock decay at both sites. We have provided pictures and concise yet informative descriptions of each sampling point in Fig. 2 and Table 1, respectively. The description includes details about the local visual aspect of the rock surface, and the extend of ongoing weathering at each site. By reporting this information, we aim to provide readers a comprehensive understanding of the specific conditions prevailing at each sampling location.

Table 1
Sampling points and their conditions as assessed by visual inspection.

Sample ID	Site	Position	Type and degree of rock decay
Y1	Yab-6	Block outside the dripline of the rock shelter	Granite block at the ground level, and displaying a moderate degree of decay due to granular disaggregation.
Y5	Yab-6	Internal wall of the rock shelter	Granite rock wall in the lower part of the rock shelter, nearby hyrax nest, covered by a yellowish, bright coating.
Y7	Yab-6	Internal wall of the rock shelter	Granite rock wall of the rock shelter displaying a moderate to high degree of decay due to exfoliation.
Y8	Yab-6	Internal wall of the rock shelter	Granite rock wall of the rock shelter displaying a moderate to high degree of decay due to exfoliation.
Y9	Yab-6	Internal wall of the rock shelter	Upper part of the granite rock wall of the rock shelter displaying a moderate to high degree of decay due to exfoliation; in the same area evidence of occasional water flow.
B1	Bor-1	Internal wall of the rock shelter	Granite rock wall of the rock shelter displaying a reddish, continuous coating on the rock and an overlapping whitish layer.
B2	Bor-1	Internal wall of the rock shelter	Granite rock wall of the rock shelter displaying a reddish, almost discontinuous coating on the rock and an overlapping whitish layer.
B7	Bor-1	Internal wall of the rock shelter	Granite rock wall of the rock shelter displaying a moderate degree of decay due to exfoliation; the rock surface is covered by an almost continuous reddish coating.

2.2. Thin section petrography and SEM-EDS

To prepare the collected rock samples for analysis, we first consolidated them in resin, then cut the resulting block perpendicular to the surface and polished it. We then manufactured thin sections that were mounted on glass slides using the protocol described in Zerboni (2008). We used an optical petrographic microscope (Olympus BX41) equipped with a digital camera (Olympus E420) to conduct a preliminary investigation of the micromorphology of the rock coatings in the thin sections. We examined the samples under both plane-polarized light (PPL) and cross-polarized light (XPL). This allowed us to obtain a detailed look at the internal structure of the samples and gain insights into the mineral composition and texture of the rock coatings. Next, we coated the thin sections with carbon and examined them using a JEOL JSM-IT500 scanning electron microscope (SEM) coupled with energy-dispersive X-ray analysis (microprobe, EDS) to conduct a chemical characterization of the samples. We used an accelerating voltage of 20 kV for this analysis. Besides the analysis of carbon-coated samples, we also

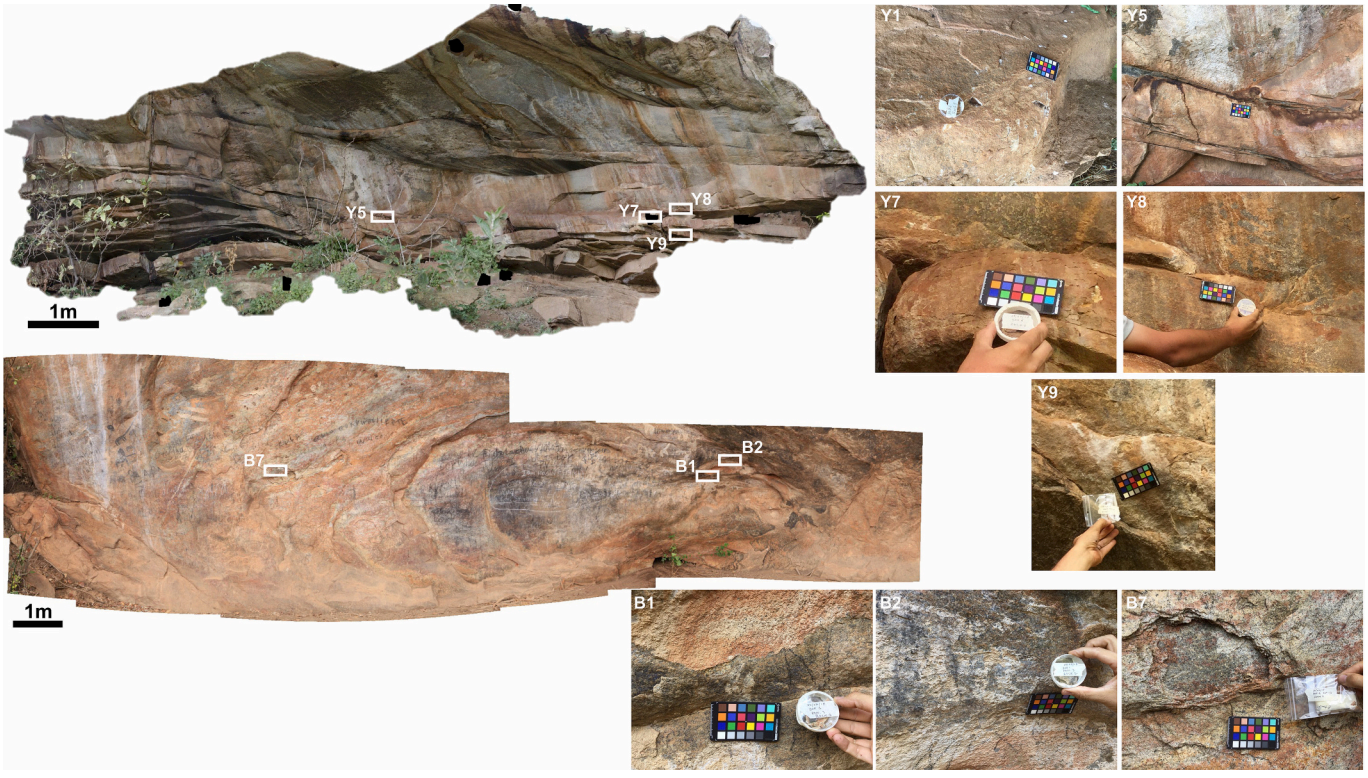

Fig. 2. The internal part of the Yabelo (upper part) and Borema (lower part) rock shelters showing the position of sampling points. The insets are details of each sampling point.

conducted additional observations on gold-covered samples to obtain high-resolution images as suggested by Gallinaro and Zerboni (2021b). Elemental concentrations measured by EDS were reported as oxide weights normalized to 100 %.

2.3. DNA extraction and sequencing

Genomic DNA was extracted using the PowerBiofilm DNA Isolation Kit (MoBio Laboratories Inc., Carlsbad, CA, USA), following the manufacturer's instructions. We conducted high-throughput sequencing analysis of the bacterial 16S rRNA gene's V3-V4 region, using the MiSeq platform (Illumina) with v3 chemistry to generate 2 × 300 paired-end reads. The primers CS1_341F and CS2_806R were used for the amplification (Rapin et al., 2017).

Raw sequencing data were processed and analyzed using QIIME2 (Bolyen et al., 2019) and DADA2 to pre-process, quality filter, trim, denoise, pair, and model the reads. Chimeric sequences were detected using the consensus method (Callahan et al., 2016), and the remaining sequences were clustered into Amplicon Sequence Variants (ASVs). Taxonomic assignments were performed using a Naïve-Bayes classifier trained on the SILVA database (Quast et al., 2013). The sequence data generated in this study have been submitted to NCBI under the BioProject ID: PRJNA988025.

2.4. Functional gene prediction

To predict the functional abundance of key bacterial genes mostly related to rock and coating interactions, energy flow, and nutrient cycling we utilized PICRUSt2 (Phylogenetic Investigation of Communities by Reconstruction of Unobserved States), which is a software package that infers metagenome functional content from 16S rRNA sequencing data (Douglas et al., 2020). Functional gene predictions were calculated from KEGG-Orthology (KO) using the Kyoto Encyclopedia of Genes and Genomes (KEGG). The enzyme data (EC numbers) and metabolism pathways of each metabolism were manually assigned based on the KEGG and BRENDA databases.

The functional genes associated with carbon fixation (pathway ko00710), nitrogen (pathway ko00910), and sulfur metabolisms (pathway ko00920) were identified based on Kyoto Encyclopedia of Genes and Genomes (KEGG) database. The functional genes related to organic P mineralization and inorganic P dissolution were selected based on the work of Liang et al. (2020) and Luo et al. (2020). The functional genes related to rock interaction were selected based on the phenomena described by Liu et al. (2020), e.g., for biosynthesis of siderophores, metal uptake/regulation, oxalate production and degradation, calcite precipitation, and inorganic acid production. The complete list of the genes investigated is reported in Table S1.

We used the following equation to normalize the gene abundance (x') belonging to the same functional group (Luo et al., 2020):

$$x' = \frac{\sum_{n=1}^{n}\left(\frac{x_i}{\sum_{i=1}^{i} x_i}\right)}{n_i}; i, n = 1, 2, 3, \ldots$$

where x_i is the individual gene abundance of the samples, i and n indicate the numbers of samples and genes studied, respectively.

To assess the impact of SABs on the underlying substrate, we selected a subset of metabolic processes that by current literature are considered to have negative or positive effects on the stone (Table 2). Subsequently, we calculated the sum of the normalized gene abundances for each level of weathering. These values were then used to determine the potential neutral, deteriorative, or protective role of the biofilm as follows:

$$\text{SAB's role} = \text{Sum of negative metabolic processes} / \text{Sum of positive metabolic processes}$$

Table 2
List of the metabolic processes selected as potentially involved in negative and positive impacts on the underlying stone according to current literature. The list of potential positive metabolic processes also includes those that may counterbalance the effects of the negative processes.

Potential negative metabolic processes		
Nitrification	Production of inorganic acid	Liu et al., 2020; Zanardini et al., 2019; Zhang et al., 2019
S oxidation	Production of inorganic acid	Li et al., 2018; Liu et al., 2020; Ren et al., 2017
Siderophore synthesis	Alteration of rock structure	Wild et al., 2022
Oxalate degradation	Removal of protective layer and alkalinization	Liu et al., 2022
Metal uptake	Alteration of rock structure	Nir et al., 2022
Inorganic P dissolution	Alteration of rock structure and acidification	Tian et al., 2021
Organic P mineralization	Acidification	Tian et al., 2021
Potential positive metabolic processes		
Denitrification	Nitrate removal process	Ding et al., 2022
Dissimilatory nitrate reduction	Nitrate removal process	Ding et al., 2022
Assimilatory nitrate reduction	Nitrate removal process	Ding et al., 2022
Dissimilatory sulfate reduction	Sulfate removal process	Qian et al., 2019
Assimilatory sulfate reduction	Sulfate removal process	Qian et al., 2019
Biomineralization	Protective layer	Gadd et al., 2014
Oxalate biosynthesis	Protective layer	Hernanz et al., 2007 Burgos-Cara et al., 2017

A ratio larger than 1 indicates that SABs play a deteriorative role. Values around 1 indicate a neutral impact. Conversely, values <1 suggest that bioprotection is the prevalent phenomenon on the stone.

2.5. Data analyses

Multi packages of R software were used to perform the statistical analyses (R Core Team, 2021). Rarefaction curves were generated using a non-normalized table of ASVs. Alpha-diversity indexes, including Richness, Shannon index, and Evenness, were calculated using multiple R software packages. To compare the bacterial community β-diversity, the Bray-Curtis distance was calculated and ordinated with the Principal Coordinate Analysis (PCoA) at the ASV level using the XLSTAT software.

The r/K selection theory was utilized to explain how bacteria adapt and optimize their fitness for survival across various weathered surfaces. In pursuit of this, we calculated the ratios between the sum of the normalized reads corresponding to K-strategists (Acidobacteriota, Actinobacteriota, and Firmicutes) and the sum of normalized reads corresponding to r-strategists (Proteobacteria, Bacteroidota, and Chloroflexi) for each level of weathering.

Sample clusters (B1; B2; Y5 low/absent weathering; B7; Y1 moderate weathering and Y7; Y8; Y) high weathering) were compared to study ASV-habitat relationship with the multinomial species classification method (CLAM), using the 'vegan' package and the function 'clamtest' in R (Chazdon et al., 2011; Pedrinho et al., 2020). The CLAM method classifies ASVs as generalists (taxa able to thrive in a wide variety of environmental conditions and resources), specialists (taxa that can thrive only in a narrow range of environmental conditions and require specific resources) for a given weathering level, or too rare to be defined. In this way, it was possible to examine the underlying ecological factors leading to the differential distribution of ASVs between weathering gradients.

The principal component analysis (PCA) was conducted on the

correlation matrix using the XLSTAT software to explore the relationship between specific functional activities and the varying degrees of weathered surfaces. Subsequently, the first two principal components (PCs) were plotted to visually depict the obtained results.

3. Results and discussion

3.1. Characterization of the stone weathering profiles

The condition of the rock surface at each sampling point revealed a range of distinct decay processes and varying overall degrees of deterioration for each sample. We have observed the development of coatings in certain cases, while weathering has resulted in exfoliation or granular disaggregation of the rock support in other samples. Table 3 provides a comprehensive summary of the primary indicators of rock decay for each sample, along with our attempt to estimate the intensity of these processes. Additionally, the table includes the presence of specific minerals or chemical compounds, based on both EDS chemical analyses and SEM images. Some areas of the rock surface exhibit no signs of mechanical weathering (absent/low weathering), while in other areas, these processes intermittently affect the rock surface (moderate weathering), or occur continuously along the entire rock surface (high weathering). Based on the abovementioned criteria, samples Y5, B1, and B2 exhibit the lowest degree of weathering, followed by samples Y1 and B7. On the other hand, samples Y7, Y8, and Y9 exhibit the highest level of decay.

In Table 4, we presented a subset of elements that are highly indicative of biological activity at the rock surface, as previously described in Dorn (1998) and Zerboni (2008). Specifically, we focused on Ca, which is associated with the presence of biogenic oxalates, phosphates, or Ca-sulfates; S, which is a marker of sulfates and may indicate the decomposition of organics; P, which is linked to the occurrence of phosphates; Fe, which indicates the precipitation of Fe-bearing oxides or hydroxides; and K and Cl, which are often found together in KCL spheroids that are associated with the decomposition of organics or excrements (see Gallinaro and Zerboni, 2021b). In Table 4, we did not include the measurement of high quantities of C and N due to the complexity of their analysis. For instance, in the case of carbon-coated samples, an excess of C can be inferred but not accurately quantified. Furthermore, additional identification of chemical compounds and neoformed minerals, likely biomineralized, was performed through SEM imaging (Fig. 3).

Based on the results of EDS chemical analyses and SEM imaging, we were able to identify several neoformed minerals in each sample, as well as biological remains such as filamentous structures. Among the most abundant minerals, we observed gypsum in a variety of crystal shapes and Ca-oxalates, which were occasionally found as well-formed euhedral crystals, rounded crystals after weathering, or as crusts covering the rock minerals.

The analyses on sample Y1 were carried out by examining both the outer and inner parts of the decaying surface. Specifically, we focused on the inner part of the rock surface, where decay products tend to accumulate along intergranular discontinuities, up to a depth of approximately 150 μm. Our findings reveal the presence of phosphates (as determined by Ca and P concentrations) and Ca-oxalates (identified visually) in the inner part of the surface. In contrast, the outer part of the coating displayed a lower concentration of phosphates. In addition, we detected occasional increases in the concentration of Fe in the same samples. These increases were interpreted as the result of the in-situ formation of Fe-oxy/hydroxides, possibly due to biomineralization after the decay of Fe-bearing rock-forming minerals.

The interpretation of chemical data obtained from the decaying surface of sample Y5 is complex, as the composition of the surface coating is likely influenced by the underlying rock-forming minerals. However, SEM imaging has provided evidence for the presence of organic features, including organic crusts. In these locations, chemical analyses have revealed an increase in the concentration of C and N.

Upon examination of sample Y7, we observed alternating concentrations of Ca from the surface to the near-surface portion of the decay

Table 3
Weathering degrees (absent/low (−), moderate (+), or high (++)) and the occurrence of minerals and chemical compounds in each sample, which was based on SEM imaging and EDS analyses. The abundance of compounds was rated as absent (−), low-medium (+), or high (++).

Sample ID	Degree of weathering	Ca-oxalates	Ca-Phosphates	Gypsum	Fe-oxy-hydroxides	K and Cl compounds	Organics (C and/or N)
Y1	+	+	++	-	+	-	+
Y5	-	+	-	-	+	+	++
Y7	++	++	-	-	-	+	-
Y8	++	++	-	-	-	-	-
Y9	++	+	++	-	+	+	+
B1	-	+	+	++	+	-	-
B2	-	+	-	++	-	-	-
B7	+	++	+	+	+	-	-

Table 4
Major elements of rock decay products that are crucial for interpreting biofilm formation and activity. The mean concentrations of these elements were detected on selected spots by EDS analysis and have been normalized to 100 % weight in oxides for accurate comparison.

Sample ID	Ca	S	P	Fe	K	Cl
Y1 (surface)	13.43	0.46	7.73	5.22	1.52	–
Y1 (surface)	10.04	0.59	6.62	6.25	2.86	–
Y1 (inner part)	33.93	1.53	25.47	1.21	0.84	–
Y1 (inner part)	36.99	0.76	29.57	6.6	0.69	–
Y1 (inner part)	41.13	0.75	33.62	1.97	–	–
Y5 (surface)	1.34	–	0.87	–	4.45	0.96
Y5 (surface)	2.57	0.68	1.57	3.63	2.76	0.39
Y5 (surface)	1.28	0.74	1.05	4.75	4.42	0.30
Y5 (surface)						
Y7 (surface)	58.71	1.30	–	–	2.23	0.59
Y7 (surface)	52.68	–	–	–	1.29	0.42
Y7 (surface)	69.27	–	–	–	2.63	0.66
Y7 (near-surface)	39.00	2.07	–	–	5.03	2.79
Y7 (near-surface)	5.48	1.11	1.16	2.70	21.37	14.84
Y7 (near-surface)	4.31	1.52	0.51	4.20	18.26	11.58
Y8 (surface)	50.78	1.36	1.31	–	1.05	0.26
Y8 (surface)	58.79	3.25	1.22	–	1.50	–
Y8 (inner part)	72.44	2.46	1.23	–	1.05	–
Y8 (inner part)	41.53	0.83	1.22	2.10	2.43	0.36
Y9 (surface)	22.16	1.04	19.14	–	6.34	0.32
Y9 (near-surface)	9.92	0.43	11.67	5.89	2.47	0.29
Y9 (near-surface)	26.07	0.67	3.15	2.63	2.52	0.20
Y9 (near-surface)	20.78	0.58	2.62	–	2.92	0.24
Y9 (inner part)	9.20	1.03	5.87	1.45	4.18	0.30
Y9 (inner part)	11.07	1.28	3.52	–	3.49	0.35
Y9 (inner part)	42.29	1.28	38.98	–	0.82	0.53
B1 (surface)	26.70	38.96	3.10	–	0.55	–
B1 (surface)	32.42	49.17	–	–	–	–
B1 (surface)	33.69	48.89	–	–	–	–
B1 (surface)	17.35	21.48	7.67	5.41	1.75	0.53
B1 (surface)	32.58	40.02	–	0.42	–	–
B2 (surface)	19.83	16.79	–	–	0.27	–
B2 (surface)	32.45	47.29	–	–	–	–
B2 (surface)	32.24	48.74	1.71	–	–	–
B2 (surface)	25.90	40.03	–	0.37	0.32	–
B2 (surface)	23.24	35.89	0.74	–	0.50	–
B2 (surface)	20.53	1.60	0.80	–	0.84	0.84
B2 (surface)	36.73	15.70	1.85	–	0.57	–
B7 (surface)	26.45	0.52	0.22	1.09	–	0.44
B7 (surface)	9.82	13.82	1.42	2.88	0.34	0.51
B7 (surface)	31.91	5.12	15.75	–	0.35	1.06
B7 (surface)	53.83	1.88	0.74	2.07	–	0.64
B7 (surface)	44.05	0.54	0.57	2.07	0.77	0.66

belt. These observations suggest the occurrence of Ca-oxalates, which were visually identified as subrounded aggregates or occasionally crusts in SEM imaging. In addition, we observed portions of the decay belt where rock-forming minerals were dotted or coated with K and Cl-rich features. These features may be related to the presence of urine residues or KCl aggregates.

Our analyses of sample Y8 revealed a large concentration of Ca, as well as high values of C. These observations suggest the common presence of Ca-oxalates within the sample. SEM imaging confirmed the presence of these minerals, which were identified as euhedral crystals or crusts.

The investigation of sample Y9 revealed a complex pattern of mineralogical variation related to weathering. At the surface, we observed the presence of phosphates, while below the phosphate-rich decay belt, we noticed an increase in Ca-oxalates. Further down, in the innermost part of the decay belt (at depths >200 μm), we found phosphates along planar discontinuities in the rock. We also observed occasional concentrations of Fe-bearing minerals in sample Y9, which we attributed to the in-situ formation of Fe-oxy/hydroxides. The EDS analyses of this sample indicated high levels of C, likely related to the occurrence of oxalates and organic matter. Interestingly, we also detected occasional concentrations of K and Cl at the very surface of the sample. These features may be related to urine residues or KCl spheroids, which we occasionally detected under SEM imaging.

The analyses conducted on the whitish crusts of samples B1 and B2 indicate that they primarily consist of gypsum. The SEM images reveal the presence of gypsum crystals with various shapes. Although occasional occurrences of phosphates were noticed in B1, they were not observed in B2. On the other hand, SEM images of the gypsum crust in B2 revealed the occasional presence of Ca-oxalate crystals coating the surface.

Sample B7 showed a variable concentration of elements, which suggests the presence of multiple minerals. Some beam points exhibit the occurrence of gypsum, while others are enriched in phosphates. A high concentration of Ca in some points indicates the presence of Ca-oxalates, which are also visible in the SEM images. The oxalates exhibit varying degrees of decay, with some crystals being well-preserved and others appearing as microcrystalline or discontinuous crusts a few microns thick.

3.2. Taxonomy diversity and trends along the weathered samples

The amount of recoverable DNA from an equivalent sample size was utilized as a rough estimation for biomass, indicating that samples with high and low degrees of weathering exhibited approximately four times less recoverable DNA compared to moderately weathered samples. Among the samples, Y1 and B7 (moderate weathering) showed the highest DNA concentration, with an average of 48.89 ± 8.85 ng/μL. In contrast, Y7, Y8, and Y9 (high weathering) samples yielded 11.96 ± 2.26 ng/μL, while Y5, B1, and B2 (low weathering) contained 7.59 ± 2.84 ng/μL. The 16S rRNA data set analyzed in this study encompassed 109,326 reads, which were clustered into 524 amplicon sequence variants (ASVs). The rarefaction curves provided confidence that the sequencing depth was adequate for a comprehensive characterization of the bacterial communities (Supplementary Fig. S1). At present, we cannot establish whether these bacterial SAB communities played a significant role in the observed weathering patterns. However, this study provides a snapshot of the current colonization and serves as an initial step to uncover the putative deterioration or protection action of SABs inhabiting the investigated rock art paintings. The bacterial communities identified in the samples were classified into 18 different phyla, encompassing a total of 142 identified genera. Notably, the composition of bacterial communities varied across the samples, with prominent phyla including Actinobacteriota (reaching up to 43 % in sample Y8), Proteobacteria (reaching up to 45 % in sample B7), Deinococcota (reaching up to 51 % in sample Y9), Firmicutes (reaching up to 87 % in sample B1) and Cyanobacteria (reaching up to 11 % in sample Y1) (Fig. 4). The recent studies conducted by Nir et al. (2019a, 2019b) on SAB communities inhabiting the dark coating layer of petroglyphs in the Negev Desert revealed three main bacterial phyla—Cyanobacteria, Actinobacteriota, and Proteobacteria— which are consistent with our results. Actinobacteriota have been found to be the dominant phylum in oligotrophic environments such as lithic surfaces and desert soil, likely due to their ability for sporulation, wide metabolic range, competitive advantages through secondary metabolite synthesis, and multiple UV repair mechanisms (Mohammadipanah and Wink, 2016; Saadouli et al., 2022). Proteobacteria are also considered significant members of bacterial communities in desert rocks and soil, particularly in nutrient-limited or dry/arid environments where they may play important

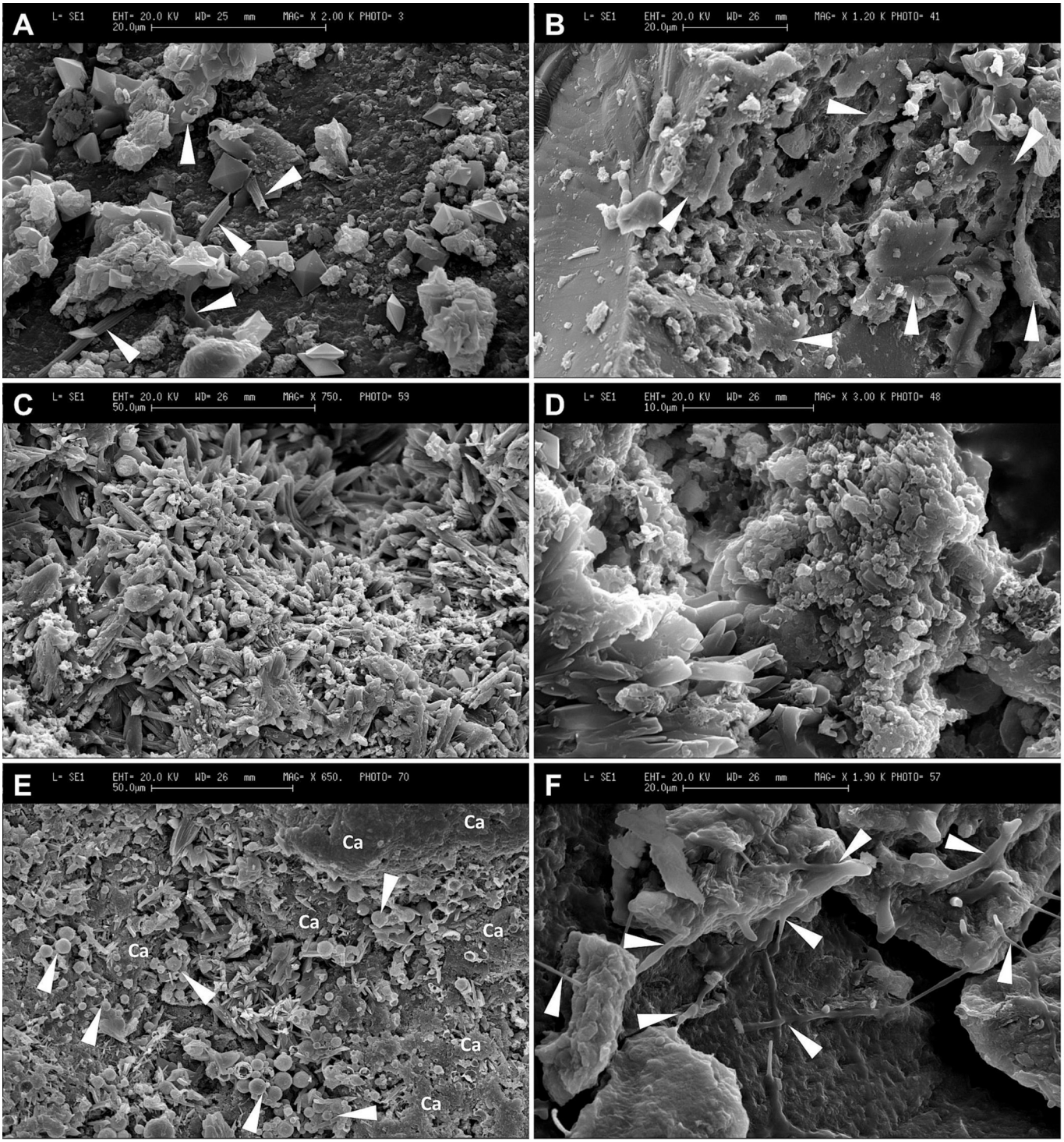

Fig. 3. Figure SEM. SEM pictures illustrate the main observed features of the samples. A) Well-preserved bipyramidal crystals of Ca-oxalate and interspersed biological remains (arrows) (sample Y7). B) A discontinuous crust of Ca-oxalates (arrows) on a quartz grain (sample Y8). C) A carpet of acicular gypsum crystals (sample B2). D) Gypsum appearing on the left as acicular crystals and on the right as a crust (sample B2). E) Concentrations of KCl spheroids (arrows) on a Ca-oxalate crust (Ca); acicular gypsum crystals are also present (sample Y8). F). Fungal hyphae (arrows) growing on crystals (sample Y7).

functional roles in fixing carbon through a bacteriochlorophyll-dependent photosynthesis (Imhoff et al., 2018). Cyanobacteria are specifically associated with biogeochemical cycles related to nitrogen or carbon utilization and stress response (Murray et al., 2022; Yadav et al., 2022).

It is noteworthy that the phyla Deinococcota and Firmicutes were found only in low percentages within those samples (Nir et al., 2022; Rabbachin et al., 2022). Nevertheless, the presence of Deinococcota and Firmicutes in stone monuments and desert varnishes is remarkable, as it underscores the adaptation of microorganisms belonging to those two phyla to the challenging environmental conditions characteristic of rock art settings (Li et al., 2018; Northup et al., 2010; Sazanova et al., 2022). These microorganisms have demonstrated their resilience and ability to thrive in harsh conditions characterized by limited nutrient availability, aridity, high salinity, temperature fluctuations, and even radiation exposure (Filippidou et al., 2016; Jin et al., 2019).

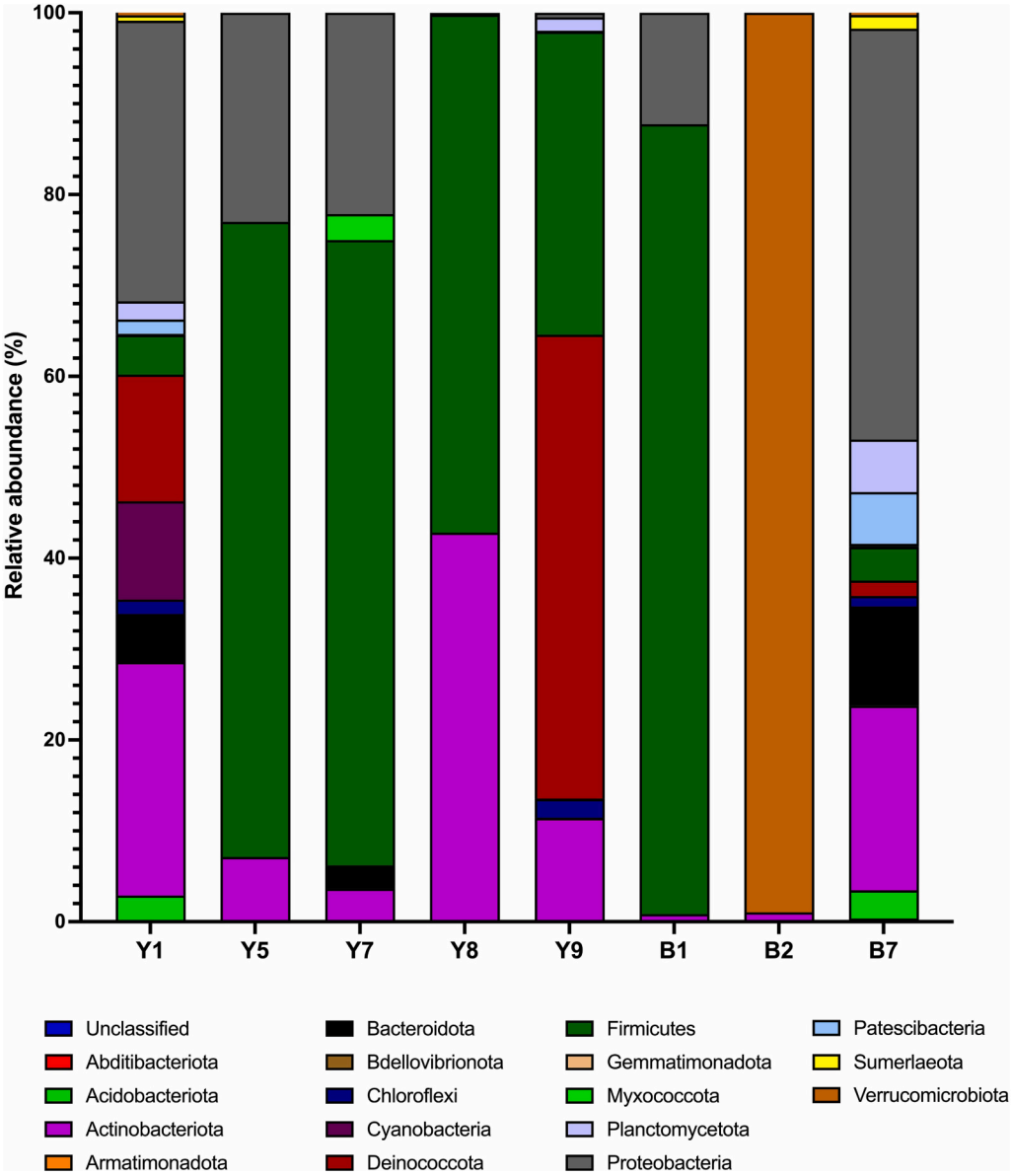

Fig. 4. Relative abundance of the dominant bacterial phyla (> 1 %) across the weathered samples.

A principal coordinate analysis (PCoA) was performed at the bacterial genus level to visualize similarities between communities across multiple samples. The principal coordinates (PCs), representing distinct portions of the observed data variability, were plotted to visually depict the compositional differences in the bacterial community among samples. The resulting PCoA plot accurately clustered the variations in bacterial community composition according to the distinct degrees of weathering identified in the geomorphological studies (Fig. 5). This observation aligns with previous studies, which have demonstrated that the microbial community structure is more strongly influenced by the chemical and physical properties of the lithic substrates, also implying the extent of weathering, rather than the prevailing climatic conditions (Brewer and Fierer, 2018; Gambino et al., 2021). Rocks provide habitats for microorganisms, and they also affect the microbial community structure (Meslier et al., 2018). Although Meslier et al. (2018) suggested that the chemical properties of the rock may not be an essential driver of community composition and diversity, the ability of microorganisms to use nutrients leached from rocks can affect the community composition in their niche. In addition, Cámara et al. (2008) suggested that the microstructure of the rock, such as the space available for colonization

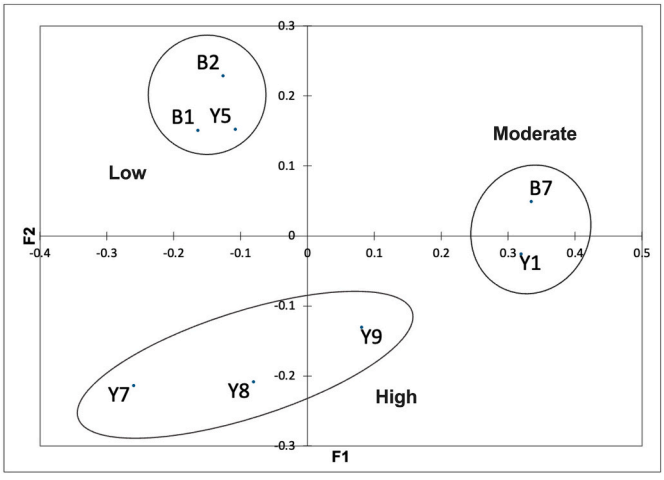

Fig. 5. β-diversity as a principal coordinate analysis (PCoA) plot based on Bray-Curtis dissimilarity.

and its physical structure, linked to water retention capabilities, can be a determinant of the potential bioreceptivity of lithic habitat.

Based on the premise that varying degrees of weathering create distinct ecological niches for microorganisms, we employed the r/K selection theory to elucidate how bacteria adapt and optimize their fitness for survival across these surfaces. The r/K selection theory finds broad applicability in describing two distinct strategist types observed in numerous natural and artificial ecosystems (Sun et al., 2021; Vadstein et al., 2018; Yin et al., 2022). The unique characteristics of r-strategists and K-strategists are crucial factors in shaping their distribution across various ecological niches. R-strategists are typically well-suited for growing in unpredictable environments characterized by fluctuating resource availability, including frequent disturbances and intermittent periods of resource abundance and scarcity. These r-strategists, known as copiotrophs, thrive by consuming readily available fresh organic matter (Akob and Küsel, 2011). In contrast, K-strategists display exceptional adaptability to stable environments where resources are limited yet consistently accessible. These K-strategists, referred to as oligotrophs, possess the ability to utilize remaining polymerized substrates, such as buried carbon, as sources of energy and nutrients (Akob and Küsel, 2011). This enables them to efficiently extract resources from low-energy environments. Taking into account the aforementioned considerations, the phyla Acidobacteriota, Actinobacteriota, and Firmicutes are typically classified as K-strategists, while Proteobacteria, Bacteroidota, and Chloroflexi are generally considered r-strategists (Chen et al., 2022; Fierer et al., 2007; Smith et al., 2022; Speirs et al., 2019). In our study, we identified a significant trend whereby the ratio K- /r-strategists decreased as the degree of weathering reached the medium level.

In contrast, the highest ratio of K- /r-strategists was observed in samples characterized by a high degree of weathering. These findings highlight a distinct pattern where r-strategists dominate in moderately weathered surfaces, while K-strategists are more prevalent in highly weathered surfaces. Lithic substrates with a moderate degree of weathering still retain significant weathering potential and undergo rapid weathering rates. This combination gives rise to the formation of diverse and fluctuating microhabitats, characterized by heterogeneity. Our geomorphological analyses have confirmed the presence of variegated and intermittent weathering processes within samples exhibiting a moderate degree of weathering, contributing to the development of a heterogeneous environment. These dynamic microhabitats, shaped by ongoing weathering processes, offer an ideal environment for r-strategists, as they thrive in unstable microenvironments with varying resource availability (Cheng et al., 2018). However, it is difficult to ascertain whether the current bacterial communities contribute to the weathering processes or if they are merely present, taking advantage of the heterogeneous surface that provides a wide range of growth substrates and conditions. Notably, our data indicated that samples displaying a moderate degree of weathering had the highest α-diversity (Supplementary Table S2). This finding aligns with the well-established understanding that habitat heterogeneity significantly influences microbial community diversity (Walters and Martiny, 2020; Zhang et al., 2020). Indeed, a heterogeneous environment plays a crucial role in shaping community composition by selectively filtering species from a species pool in diverse ways across local communities (Dini-Andreote et al., 2015). This selective process ultimately leads to the emergence of a high α-diversity (Dini-Andreote et al., 2015), highlighting the profound influence of habitat heterogeneity on microbial communities.

In contrast, high-weathering degree samples, as indicated by our findings, displayed uniform mechanical weathering, leading to a more homogeneous environment within a sample. Thus, extensively weathered lithic substrates exhibited a more stabilized microenvironment with limited resource supplies. This stabilized and homogeneous environment provides favorable conditions for the development of K-strategists. In a recent study by Chen et al. (2022) an intriguing finding was reported regarding the weathering of carbonatite over time. It was observed that microbial taxa at the phylum level underwent a gradual transition from r-strategists to K-strategists, indicating a shift from copiotrophs to oligotrophs as the weathering process advanced. It was evident that samples with a high degree of weathering exhibited lower α-diversity when compared to those with a moderate weathering rate. This contrast in α-diversity can be attributed to the distinct effects of heterogeneous and homogeneous environments. While a heterogeneous environment selectively filters species in diverse manners, promoting higher α-diversity, a homogeneous environment filters species in a similar manner, resulting in lower α-diversity. Collectively, our findings reinforce the concept that habitat heterogeneity plays a crucial role in influencing bacterial diversity, as the observed patterns of r/K-strategists and α-diversity align with the niche variability present across the different weathered samples. This observation aligns with similar findings from surface soil and rock habitats in hot and cold deserts, where the physical environment's role in niche filtering is crucial for microbial community assembly (Lee et al., 2016; Rolli et al., 2022).

To identify family-level ASVs that displayed preferential associations with different degrees of weathering, we employed the CLAM test (Chazdon et al., 2011) for multinomial species classification. This method categorizes the ASVs into three distinct groups based on their distribution among samples: ASVs that exhibited a clear preference for a specific weathering degree (specialists), ASVs that showed no discernible preference (generalists), and ASVs that were too rare to confidently classify (rare). Thus, we conducted a comparative analysis of niche occupancy across various samples by assessing the proportions of generalist and specialist microorganisms (Fig. 6). This analysis involved determining the percentage of microorganisms that demonstrated a broad ecological range (generalists) compared to those with a narrower ecological range (specialists). Across all three degrees of weathering, we observed a higher proportion of specialist microorganisms compared to generalists. Remarkably, the percentage of specialist microorganisms reaches its peak in samples characterized by moderate weathering, demonstrating the highest level of specialization.

In contrast, samples with low weathering exhibit the lowest percentage of specialist microorganisms. This finding underscores the adaptation of bacterial communities to specific abiotic conditions, indicating that a larger percentage of microorganisms have developed specialized traits tailored to thrive under particular weathering conditions. The results provide compelling evidence for the heightened specialization of microorganisms as the weathering intensity progresses. The majority of bacteria associated with low weathering degrees were found to belong to the families Akkermansiaceae, Aerococcacee, Lactobacillaceae, Staphylococcaceae, and Streptococcaceae. The families Bacillaceae, Brevibacteriaceae, Planococcaceae, Carnobacteriaceae, Clostridia, Planococcaceae, and Rubrobacteriaceae were found to harbor a significant number of ASVs favored by high weathering levels. On the other hand, the families Burkholderiaceae, Chroococcidiopsaceae, Intrasporangiaceae, Rhodobacteraceae, Saccharimonadales, and Xanthomonadaceae emerged as specialists associated with samples exhibiting moderate levels of weathering.

3.3. Potential functional pathways in microorganisms across various weathering profiles

In this research, we investigated the structure and predicted functions of bacterial assemblages in SABs and examined their relationships with varying degrees of stone weathering that impact southern Ethiopian rock paintings. We also assessed the net impact of the bacterial communities on the underlying stone by analyzing the ratios between specific metabolic processes associated with biodeterioration (e.g., nitrification, metal uptake, oxalate degradation) and those that counteract the biodeteriorative effects (e.g., denitrification, assimilatory and dissimilatory nitrate reduction) or play a protective role themselves (e.g., oxalate biosynthesis, calcite precipitation). The attribution of positive and negative effects has been done according to current literature. It

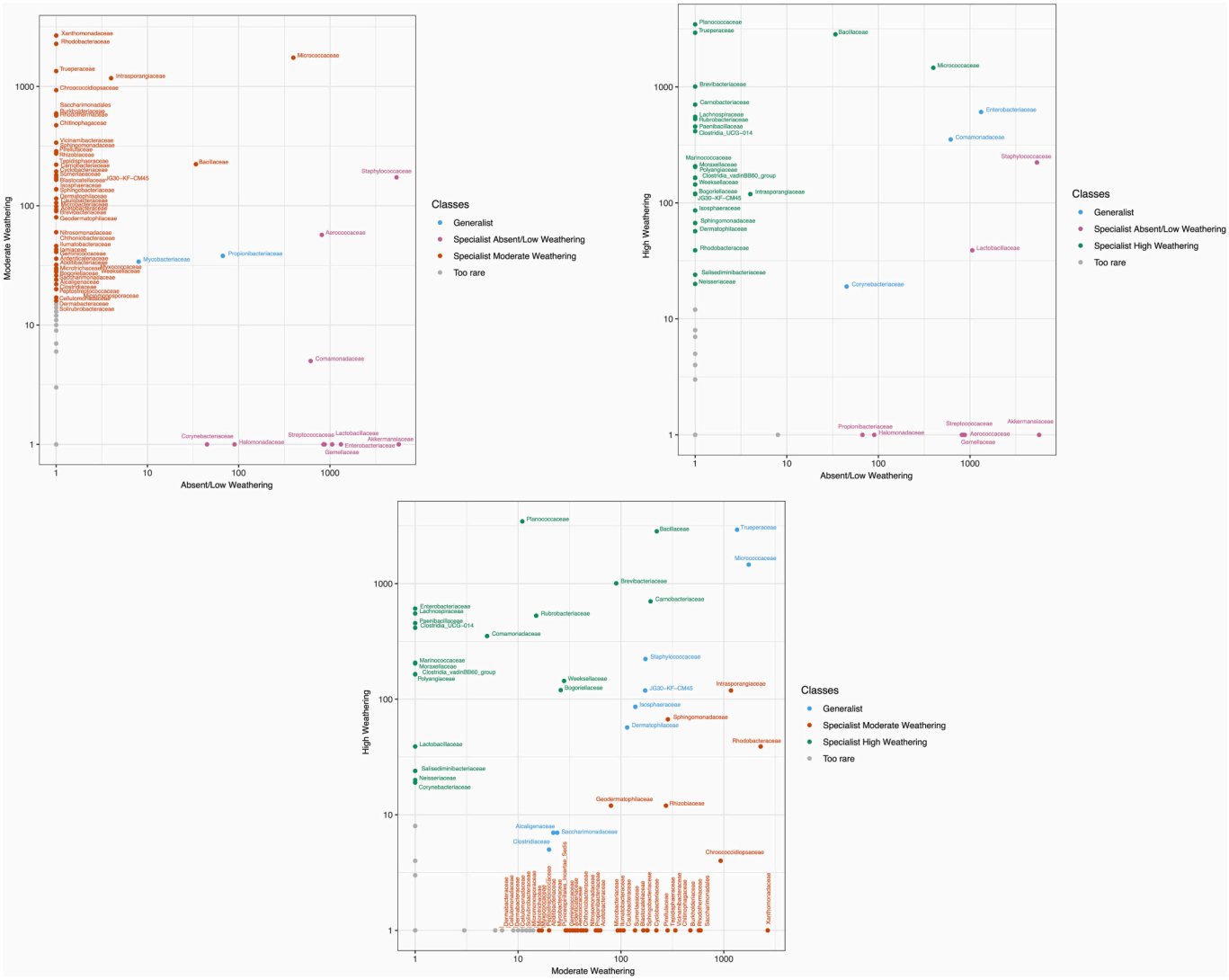

Fig. 6. Multinomial species classification method (CLAM) test signifying the Absent/Low weathering (pink), Moderate weathering (orange), and High weathering (green). Generalist families are reported in blue. ASVs that were too rare to classify are shown in light gray.

is worth noting that microbial deterioration has been extensively studied whereas biofilm protection studies are still in their infancy.

The functional content was determined by analyzing marker genes associated with key element cycles, carbon fixation, stress response, and other relevant processes using PICRUSt2. PICRUSt is a predictive method that takes into account the phylogenetic tree and the distance to the closest functionally annotated reference microorganism. However, a significant limitation of PICRUSt arises when dealing with 16S sequences, as they may lack sequenced/annotated genomes of phylogenetically close relatives in the reference database (Langille, 2018). Furthermore, these genes may not undergo transcription or translation, thereby restricting the reliability of their annotated function (Das et al., 2020). Consequently, the microbiome functions derived from PICRUSt should be considered as potential, requiring further validation through functional assays. Although our approach reflects potential rather than realized functional capacity, the obtained data provide valuable insights into the poorly understood metabolism of bacterial communities inhabiting southern Ethiopian rock art painting. We evaluated the importance of each metabolic pathway by using the relative abundance of predicted functional genes as a proxy (Please see Supplementary Table S1). The heatmap depicted in Fig. 7A illustrates the trends of predicted functional genes across the various samples, while the PCA plot presented in Fig. 7B highlights the specific functional activities associated with different degrees of weathered surfaces. Notably, the first axis of the PCA plot discriminates the primary metabolic activities observed in samples with low and moderate degrees of weathering, while the second axis represents the functional characteristics of bacterial communities residing in highly-weathered surfaces.

3.4. Carbon fixation

In oligotrophic environments, such as those represented by stone monuments and rock art, carbon fixation is a major challenge, particularly in unpolluted areas. Of the 6098 predicted genes, 26 functional genes were associated with carbon fixation pathways in photosynthetic bacteria (from 0.7 % to 1 % of the whole data set) and 67 with carbon fixation pathways in prokaryotes (from 1.3 % to 1.9 % of the whole data set).

Samples exhibiting moderate weathering degrees showed the greatest potential for carbon fixation compared to samples characterized by high and low weathering levels. The analysis confirmed that key genes involved in Calvin-Benson-Bassham (CBB) cycle, namely ribulose-1,5-biphosphate carboxylase/oxygenase (RuBisCO) large (K01601) and small (K01602) chain, were attributed to Cyanobacteria, Proteobacteria, and Actinobacteriota. Proteobacteria have the ability to undergo bacteriochlorophyll-based anoxygenic photosynthesis (Imhoff et al.,

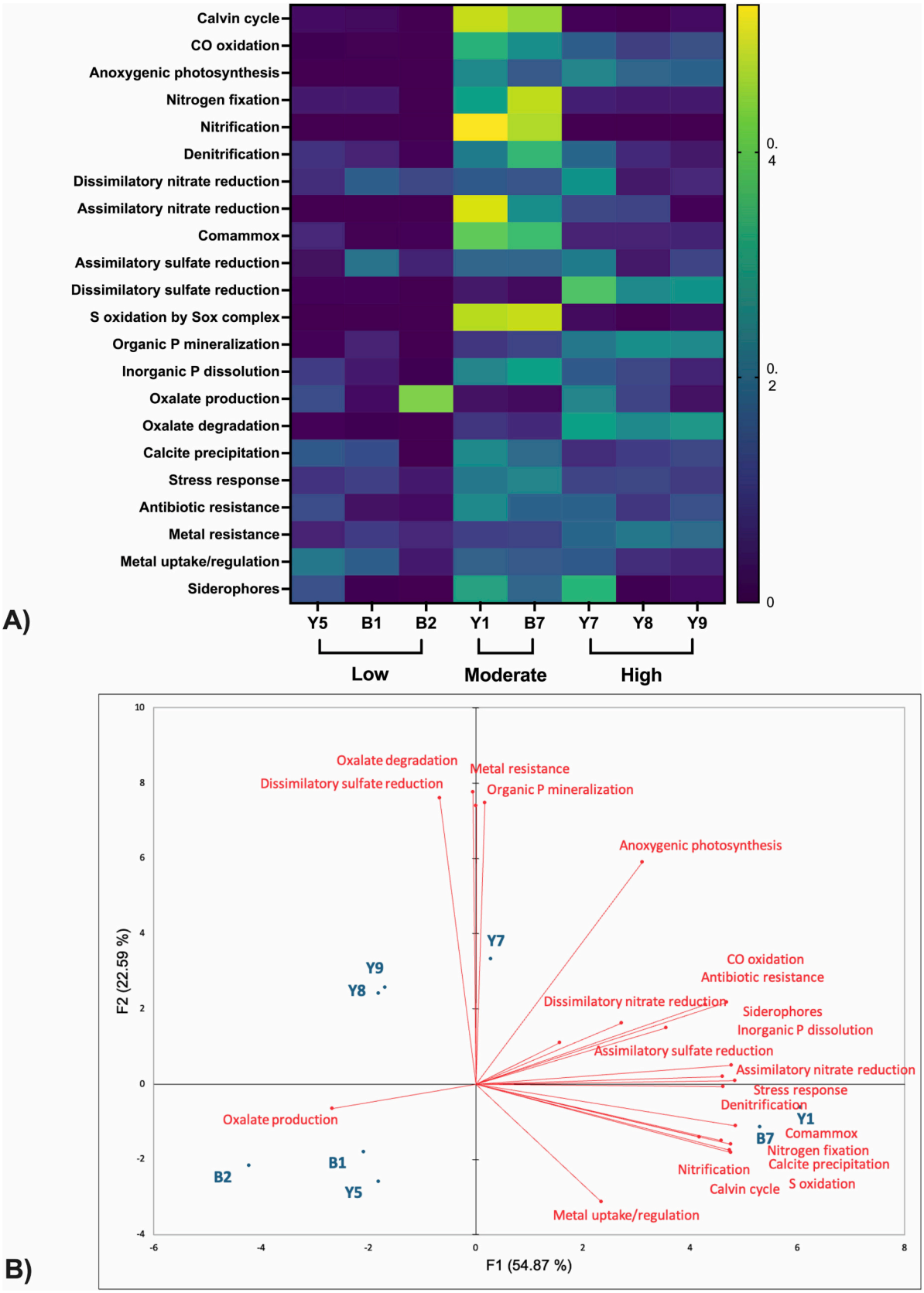

Fig. 7. A) Heatmap profiles showing the functional categories of bacterial communities as predicted by PICRUSt2. B) PCA biplot showing the relationship among samples and the predicted metabolic functions.

2019). However, their role in carbon fixation is often overshadowed when compared to the more recognized cyanobacterial oxygenic photosynthesis. In samples with moderate weathering degrees, we inferred genes involved in bacteriochlorophyll synthesis (*bch*G and *bch*Y,) as well as genes for the photosynthetic reaction center of the anoxygenic photosystem (*puf*M and *puf*L) associated with the Proteobacteria phylum.

Members of the phyla Proteobacteria and Actinobacteriota are chemoheterotrophs that can also support carbon fixation by oxidizing atmospheric trace gases (Greening and Grinter, 2022). Our analysis predicted that both Proteobacteria and Actinobacteriota harbored genes for trace gas scavenging (e.g., carbon-monoxide dehydrogenase, *cox*L), and the electrons obtained from these oxidations were proposed to act in conjunction with RuBisCO to support carbon fixation through the CBB cycle (Ray et al., 2022). It has been demonstrated that soil microbial communities are capable of aerobically respiring carbon monoxide by using the enzyme carbon monoxide dehydrogenase, which is induced during carbon limitation and enhances survival in conditions of starvation (Cordero et al., 2019; Patrauchan et al., 2012). Several bacterial phyla have been found to scavenge atmospheric CO, including Actinobacteriota (King and Weber, 2007), Proteobacteria (King, 2003) and Chloroflexi (Islam et al., 2019). Furthermore, recent advancements in genomic research have led to the identification of putative CO dehydrogenase genes in an impressive range of 16 microbial phyla, further expanding our understanding of the widespread occurrence of this vital metabolic trait (Cordero et al., 2019). Biochemical studies have demonstrated that soils possess the capability to oxidize atmospheric H_2 and CO at rates that can theoretically meet the energy requirements of their microbial communities (Ji et al., 2017). Furthermore, studies conducted on pure cultures consistently indicate that scavenging of trace gases enables the survival of various heterotrophic aerobes when they experience organic carbon deprivation (Greening et al., 2015). Thus, atmospheric chemosynthesis is a globally-distributed phenomenon that spans cold and hot deserts worldwide, yielding far-reaching implications for the global carbon cycle and the survival of bacteria within environmental reservoirs (Bay et al., 2021; Ray et al., 2022).

We also predicted key genes associated with the reductive citric acid cycle (Arnon-Buchanan cycle), the reductive acetyl-CoA pathway (Wood-Ljungdahl pathway), and the 3-hydroxypropionate bicycle across all samples.

Collectively, the predicted metagenome data indicate that in samples with moderate weathering degrees, SAB communities have the greatest potential for carbon fixation through a combination of photosynthetic and chemosynthetic processes. The potential primary productivity observed in samples with moderate weathering degrees plays a vital role in supporting the substantial bacterial biomass and biodiversity observed within these samples.

3.5. Nitrogen, sulfur, and phosphorus metabolisms

As low-biomass microbial communities, stone microbiomes require the inherent ability to be self-sustaining, primarily through the efficient cycling of essential elements like nitrogen, sulfur, and phosphorus (Zanardini et al., 2019).

Genes involved in six nitrogen metabolism pathways including nitrogen fixation, nitrification, denitrification, cammamox, assimilatory, and dissimilatory nitrate reduction pathways, were predicted in the metagenomes of the samples. Interestingly, only samples with moderate weathering degrees showed a complete nitrogen cycle. These samples harbor bacterial communities with the highest genetic potential for nitrogen fixation, nitrification, complete ammonia oxidation (cammamox), denitrification, and assimilatory nitrate reduction. In contrast, high and low-weathered surfaces completely missed genes for nitrification, while retaining capacities for the cammamox process. Previous studies of SAB communities inhabiting deteriorated stone monuments have revealed the presence of nitrifying bacteria and archaea (Ding et al., 2021, 2022). The process of nitrification, which produces nitrate and potentially nitric acid, has been proposed as a contributing factor to the deterioration of stone materials (Liu et al., 2020; Zanardini et al., 2019; Zhang et al., 2019). Moreover, two recent studies suggested that microorganisms associated with biodeterioration, such as nitrogen cycling-associated bacteria, exhibit insensitivity to antimicrobials or can even metabolize them (Ding et al., 2022; Wang et al., 2021).

It is important to note that genes associated with nitrate removal processes, namely denitrification, assimilatory nitrate reduction, and dissimilatory nitrate reduction, were predicted in all samples exhibiting moderate degrees of weathering. This indicates that the bacterial community present on moderately deteriorated surfaces possesses the potential capability to remove harmful inorganic acids generated by the activity of nitrifying bacteria. However, previous research has shown that the removal of nitrate is weak or undetectable on stone monuments, indicating that these microbial communities may not effectively eliminate the accumulated nitrate (Ding et al., 2021, 2022). Furthermore, the process of dissimilatory nitrate reduction to ammonium serves not only to reduce the concentration of nitrate but also simultaneously supplies a constant flow of ammonia as a substrate for nitrifying microorganisms. The dissimilatory nitrate reduction to ammonia is an energy-yielding process that can retain the biologically useable NH_4^+ in the system for further biological processes. This internal recycling of ammonia and nitrate plays a pivotal role in facilitating the accumulation of biomass on stone surfaces (Ding et al., 2021). Additionally, it contributes to the alteration of substrate properties, including dissolution, through biochemical reactions. In addition, nitrifying bacteria incorporate CO_2 into biomass that immobilizes on the stone surfaces (Ding et al., 2022). As a result, the immobilization of biomass leads to modifications in the physical properties of the stone, particularly in terms of porosity and water-holding capacity. These alterations subsequently are supposed to enhance degradation reactions impacting the rock and contribute to the diversification of the microbial diversity (Qian et al., 2022).

By examining the predicted metagenomes, we found a network of sulfur compound conversions, which encompass assimilatory and dissimilatory sulfate reduction, sulfur mineralization, and sulfur oxidation in all the samples. In the S cycle, the predominant gene in moderately-weathered samples aligns with the assimilatory sulfate reduction pathway and sulfur/thiosulfate oxidation processes by the Sox complex. Assimilatory sulfate reduction, commonly observed in numerous anoxygenic phototrophic bacteria, plays a crucial role in the biosynthesis of sulfur-containing compounds. This suggests that microbial assemblages within moderate-deteriorated stone samples prioritize inorganic sulfur as a source for biosynthesis rather than an electron acceptor. By contrast, the predicted metagenomes of samples with high weathering degrees were mainly characterized by the dissimilatory sulfate reduction pathways, a key metabolic process used for energy conservation that produces sulfide.

The Sox system is a multienzyme pathway responsible for catalyzing the oxidation of hydrogen sulfite, thiosulfate, elemental sulfur, and sulfite to form sulfur intermediates or sulfate. The ability to oxidize sulfur compounds is a characteristic observed in various phylogenetically diverse bacteria, including chemolithotrophic members belonging to the phyla Proteobacteria, Firmicutes, and Actinobacteriota (Friedrich et al., 2001; Kusumi et al., 2011). The presence of specific genes responsible for catalyzing sulfur oxidation in bacteria implies that their activity could potentially contribute to the generation of acidity, which, in turn, can impact the mineral formation and stability (Li et al., 2018; Liu et al., 2020; Ren et al., 2017). Sulfur-oxidizing bacteria that excrete sulfuric acid were the dominant group of microorganisms involved in exfoliate weathering of sandstone at the Angkor site (Ding et al., 2022; Li et al., 2008).

In P-limited environments, such as lithic substrates, the ability of microbes to solubilize persistent phosphorus compounds play a crucial role in their adaptation and survival within these habitats. Microbes employ a set of enzymes derived from their metabolic processes to

release free orthophosphate from recalcitrant organic P forms. These enzymes include alkaline phosphatase (*phoD*), phytase (*appA*), phosphonatase (*phnX*), and C—P lyase (*phnJ*) (Liang et al., 2020). By utilizing these enzymes, microbes can break down complex organic P compounds, liberating orthophosphate that can be readily utilized as a nutrient source. Furthermore, glucose dehydrogenase (gcd), inorganic pyrophosphatase (*ppa*), and pyrroloquinoline-quinone synthase (*pqqC*) are additional microbial enzymes involved in the solubilization of recalcitrant inorganic P forms (Liang et al., 2020; Luo et al., 2020). Altogether, these enzymes aid in the breakdown of complex organic and inorganic P compounds, enabling the release of available orthophosphate for microbial utilization. Samples with moderate weathering degrees showed the highest relative percentage of genes implicated in the inorganic P dissolution, while high-weathered samples are characterized by the capacity to mineralize organic P. In both cases, the bacterial communities displayed the potential role of affecting the rock structure and promoting its degradation over time through the transformation of phosphorus compounds (Tian et al., 2021). Additionally, inorganic phosphorus dissolution can affect rock by altering the pH of the surrounding environment. Changes in pH can impact the solubility of other minerals present in the rock, leading to the formation of secondary mineral phases. In our study, members of the phylum Actinobacteriota were involved in the inorganic P dissolution. Actinobacteria, especially *Streptomyces* and *Micromonospora*, mineral phosphate-solubilizing have the ability to promote nutrient availability and cycling in soil ecosystems (Farhat et al., 2015).

3.6. Stress response, antimicrobial resistance, and interactions with minerals

Almost nothing is known about the stress response in bacterial communities inhabiting rock art. This study has provided unique evidence that reveals the presence of a variety of potential stress response pathways in SAB communities, spanning different niches. These pathways consist of specific genes and σ-factors that enable the bacteria to respond to various stressors, including osmotic, oxidative, heat shock, and nutrient stress. All samples analyzed in this study showed the signature of genes encoding stress resistance and damage repair mechanisms. Chaperone genes *groEL* and *dnaK*, along with the DNA repair gene *recA*, were predicted to be highly abundant in the bacterial communities analyzed. Additionally, the relative abundances of catalase genes (*katE* and *KatG*) and the presence of the RpoS regulatory system further reinforce the prevailing understanding that microbial cells in hot desert environments primarily experience stress induced by radiation and desiccation, particularly those associated with oxidation processes (Jeong et al., 2016; Schellhorn, 2020). Notably, the samples exhibiting the highest genetic potential for stress response were found in relation to moderate weathering degrees, followed by samples with high weathering levels, and finally, samples with low weathering levels.

By contrast, high-weathered samples were those with the highest relative abundance of metal resistance genes. A recent work carried out by He et al. (2022) revealed that the microbiota present in stones harbors a wide range of antimicrobial resistance genes, including those associated with antibiotics, biocides, and metals. These findings emphasized that stones could serve as natural reservoirs of the resistome, where antimicrobial resistance genes are acquired through species turnover and genetic element transfer (He et al., 2022). Therefore, the potential use of biocides to remove the rock microbiome should be carefully considered (Villa et al., 2020).

We also investigated the genetic potential of the bacterial communities to interact with lithic substrates by examining genes involved in various processes such as oxalate formation and degradation (Liu et al., 2020, 2022), calcite precipitation (Liu et al., 2020, 2022), metal uptake and regulation (Adamo and Violante, 2000; Nir et al., 2022), and synthesis of siderophores (Varliero et al., 2021; Wild et al., 2022). The predicted metagenomes revealed that the oxalate degradation pathway was predominantly associated with high-weathered samples while oxalate biosynthesis was characterized mainly by low-weathered samples. Oxalate-rich coatings, often found in rock shelters, offer not only crucial opportunities for radiocarbon dating of associated rock art (Green et al., 2021) but also protection of prehistoric paintings (Hernanz et al., 2007). Therefore, the removal of these coatings would not be desirable. The oxidation of oxalates by oxalotrophic bacteria leads to an increase in alkalinity, causing the surrounding environment to reach a pH of >9, thereby enabling the precipitation of calcite (Gadd et al., 2012). Thus, the oxidation and degradation of calcium oxalates can facilitate the formation of calcium carbonate, which, in turn, has the potential to further solidify and cement preexisting limestones by filling pores with recrystallized calcite (Gadd et al., 2012, 2014). Oxalate plays a pivotal role in complexing or precipitating metals as secondary biominerals, which can have dual consequences of mineral dissolution or metal immobilization. Additionally, oxalate exhibits metal-reducing properties, effectively reducing metals like Mn(IV) to Mn(II) (Ferrier et al., 2022; Wei et al., 2012). Oxalates have been implicated in the mobilization of various elements, including Fe, Si, Mg, Ca, K, and Al, from diverse rock formations such as sandstone, basalt, granite, calcareous rocks, and silicates (Gadd et al., 2014; González-Gómez et al., 2018). Thus, the oxidation and degradation of oxalates can have important implications for the speciation and mobility of heavy metals (Syed et al., 2020), with consequences for the rock microbiome (Sazanova et al., 2022). As a consequence, it is not surprising to observe the genetic potential of heavy metal-tolerant microorganisms in samples with high weathering degrees. Signatures of genes involved in the uptake and regulation of metal ions can serve as indicators of processes related to the extraction and absorption of ions from rocks (Nir et al., 2022; Potysz and Bartz, 2022). These genetic markers may provide insights into material deterioration processes, as recently indicated in petroglyphs from the Negev Desert, Israel (Nir et al., 2022). The presence of genes associated with siderophore metabolism indicates the necessity for high siderophore production to facilitate the uptake of iron released during rock dissolution processes (Buss et al., 2007; Perez et al., 2016; Torres et al., 2014). Thus, the production of siderophores by bacteria is considered a key factor in enhancing the leaching of mineral elements (Potysz and Bartz, 2022).

The assessment of metabolic processes that potentially influence the underlying stone (Table 2) aimed to gauge the overall impact of the bacterial community on the lithic substrate. Using the proposed equation 'SAB's role = Sum of negative metabolic processes/Sum of positive metabolic processes', the potential net effect of the bacterial community was found to be protective on low-weathered surfaces (0.50), deteriorative on medium-weathered surfaces (1.43), and neutral on high-weathered surfaces (0.91). Hence, it appears that the bacterial community inhabiting lithic substrates with a moderate degree of weathering retains the potential for a negative impact on the stone, indicating that the weathering process on these surfaces is likely ongoing. Recently, Liu et al. (2022) introduced the 'relative bioprotection ratio', defined as the ratio between the sum of natural weathering and the sum of biodeterioration. However, it was not clear how to quantify the natural weathering or the biodeterioration. In this paper, we presented the first attempt to quantify the role of biofilms by examining the co-occurrence of protection and deterioration through the predicted metabolic capabilities of the bacterial communities. This approach allowed us to determine whether protection or deterioration predominantly influences the net effects.

4. Conclusion

In order to obtain a thorough comprehension of microbial processes and their influence on rock art conservation, it is vital to delve into both the structure and functions of the microbial ecosystem. Thanks to high-throughput molecular technologies and advanced bioinformatics tools, we are now able to predict the functional capabilities of microbial

communities.

This study presents the first comprehensive investigation of bacterial communities associated with southern Ethiopian rock art paintings. Through taxonomic and predictive functional analyses of SAB communities, we established a correlation between the bacterial microbiome found in rock paintings and the varying degrees of weathering observed in the lithic substrates. Moreover, for the first time, we conducted an analysis of the bacterial communities' effect on the underlying stone. By carefully examining the interplay between negative and positive metabolic processes, which have been recognized as biodeteriorative or bioprotective in prior research, we could discern the net impact of these communities on the substrate.

The present study revealed that samples experiencing both low and high levels of weathering reached a climax stage, characterized by stable and uniform microenvironments with limited resource availability. This condition not only led to the predominance of K-strategist microorganisms—commonly known as oligotrophic bacteria— and reduced α-biodiversity but also fostered the selection of bacterial communities that exerted a positive or neutral impact on the substrate. In contrast, samples featuring moderately-weathered surfaces displayed diverse and fluctuating microhabitats, characterized by significant heterogeneity. This condition contributed to the selection of r-strategist bacteria, commonly known as copiotrophic bacteria. As a result, there was an increase in α-biodiversity and a higher percentage of specialist microorganisms compared to samples with low and high weathering degrees. From the metabolic point of view, the bacterial communities residing in moderately-weathered samples exhibited the greatest genetic potential for carbon fixation and stress responses. Additionally, these communities demonstrated a complete nitrogen and sulfur cycle and had the potential to negatively impact the underlying stone. Therefore, moderately-weathered surfaces are likely to retain substantial weathering potential, and as the weathering intensity advances, they experience increased specialization of microorganisms.

In conclusion, this study provides evidence that SABs on surfaces with different degrees of weathering host unique bacterial communities with distinct metabolic profiles. The metabolic functions play a critical role in fostering mineral-microorganism interactions and promoting the adaptability of bacteria within the diverse ecological niches shaped by the weathering processes.

While DNA-based investigations primarily reveal the potential rather than the actual functional capacity, our data offer valuable insights into the metabolisms of bacterial communities colonizing rock art paintings. This research sheds light on the potential dynamics between bacterial ecology and stone weathering, a vital insight for developing effective conservation strategies that leverage the positive aspects of biofilms while addressing their negative consequences. Future works will be devoted to studying microbial community transcriptomes to identify the active members and metabolic processes of the stone microbiome.

Supplementary data to this article can be found online at https://doi.org/10.1016/j.scitotenv.2023.168026.

CRediT authorship contribution statement

Gianmarco Mugnai: Investigation, Formal analysis, Visualization, Data curation, Writing – original draft, Writing – review & editing. **Luigimaria Borruso:** Investigation, Formal analysis, Visualization, Data curation, Writing – original draft, Writing – review & editing. **Ying-Li Wu:** Methodology, Investigation, Formal analysis, Writing – review & editing. **Marina Gallinaro:** Conceptualization, Methodology, Investigation, Writing – review & editing, Resources. **Francesca Cappitelli:** Conceptualization, Methodology, Writing – review & editing. **Andrea Zerboni:** Conceptualization, Methodology, Investigation, Formal analysis, Writing – review & editing, Resources, Supervision. **Federica Villa:** Conceptualization, Methodology, Investigation, Writing – original draft, Writing – review & editing, Resources, Supervision.

Declaration of competing interest

The authors declare that they have no known competing financial interests or personal relationships that could have appeared to influence the work reported in this paper.

Data availability

Data will be made available on request.

Acknowledgments

The Ethiopian Heritage Authority (EHA, formerly ARCCH) granted to M.G. (PI of the project) all necessary permits for sampling, exportation, and analyses of samples. We wish to thank the Ethiopian Heritage Authority in Addis Ababa, the Italian Ministry for Foreign Affairs, the Italian Institute of Culture in Addis Ababa, and the Borana Zone Culture and Tourism Office for their continuous support. Field activities in Ethiopia have been supported by the Italian Ministry of Foreign Affairs (entrusted to M.G.). This research is also part of the ASArt-DATA project funded by the European Union's Horizon 2020 research and innovation program under the Marie Skłodowska-Curie grant agreement No. 795744. Scientific analyses were supported by the CHROMA Project (SEED 2019 Grant from the University of Milano entrusted to A.Z.). The Ph.D. of Y.-L.W. was funded by the Ministry of Education in Taiwan. Part of this research was supported by the Italian Ministry of Education, University, and Research (MIUR) through the project 'Dipartimenti di Eccellenza 2018–2022' (WP4–Risorse del Patrimonio Culturale) awarded to the Dipartimento di Scienze della Terra 'A. Desio' of the Università degli Studi di Milano.

References

Adamo, P., Violante, P., 2000. Weathering of rocks and neogenesis of minerals associated with lichen activity. Appl. Clay Sci. 16, 229–256. https://doi.org/10.1016/S0169-1317(99)00056-3.

Akob, D.M., Küsel, K., 2011. Where microorganisms meet rocks in the Earth's critical zone. Biogeosciences 8, 3531–3543. https://doi.org/10.5194/bg-8-3531-2011.

Andreae, M.O., Al-Amri, A., Andreae, T.W., Garfinkel, A., Haug, G., Jochum, K.P., Stoll, B., Weis, U., 2020. Geochemical studies on rock varnish and petroglyphs in the Owens and Rose Valleys. California. PLoS One 15, e0235421. https://doi.org/10.1371/journal.pone.0235421.

Bay, S.K., Waite, D.W., Dong, X., Gillor, O., Chown, S.L., Hugenholtz, P., Greening, C., 2021. Chemosynthetic and photosynthetic bacteria contribute differentially to primary production across a steep desert aridity gradient. ISME J. 15, 3339–3356. https://doi.org/10.1038/s41396-021-01001-0.

Bolyen, E., Rideout, J.R., Dillon, M.R., Bokulich, N.A., Abnet, C.C., Al-Ghalith, G.A., Alexander, H., Alm, E.J., Arumugam, M., Asnicar, F., Bai, Y., Bisanz, J.E., Bittinger, K., Brejnrod, A., Brislawn, C.J., Brown, C.T., Callahan, B.J., Caraballo-Rodríguez, A.M., Chase, J., Cope, E.K., Da Silva, R., Diener, C., Dorrestein, P.C., Douglas, G.M., Durall, D.M., Duvallet, C., Edwardson, C.F., Ernst, M., Estaki, M., Fouquier, J., Gauglitz, J.M., Gibbons, S.M., Gibson, D.L., Gonzalez, A., Gorlick, K., Guo, J., Hillmann, B., Holmes, S., Holste, H., Huttenhower, C., Huttley, G.A., Janssen, S., Jarmusch, A.K., Jiang, L., Kaehler, B.D., Kang, K.B., Keefe, C.R., Keim, P., Kelley, S.T., Knights, D., Koester, I., Kosciolek, T., Kreps, J., Langille, M.G.I., Lee, J., Ley, R., Liu, Y.-X., Loftfield, E., Lozupone, C., Maher, M., Marotz, C., Martin, B.D., McDonald, D., McIver, L.J., Melnik, A.V., Metcalf, J.L., Morgan, S.C., Morton, J.T., Naimey, A.T., Navas-Molina, J.A., Nothias, L.F., Orchanian, S.B., Pearson, T., Peoples, S.L., Petras, D., Preuss, M.L., Pruesse, E., Rasmussen, L.B., Rivers, A., Robeson, M.S., Rosenthal, P., Segata, N., Shaffer, M., Shiffer, A., Sinha, R., Song, S.J., Spear, J.R., Swafford, A.D., Thompson, L.R., Torres, P.J., Trinh, P., Tripathi, A., Turnbaugh, P.J., Ul-Hasan, S., van der Hooft, J.J.J., Vargas, F., Vázquez-Baeza, Y., Vogtmann, E., von Hippel, M., Walters, W., Wan, Y., Wang, M., Warren, J., Weber, K. C., Williamson, C.H.D., Willis, A.D., Xu, Z.Z., Zaneveld, J.R., Zhang, Y., Zhu, Q., Knight, R., Caporaso, J.G., 2019. Reproducible, interactive, scalable and extensible microbiome data science using QIIME 2. Nat. Biotechnol. 37, 852–857. https://doi.org/10.1038/s41587-019-0209-9.

Brewer, T.E., Fierer, N., 2018. Tales from the tomb: the microbial ecology of exposed rock surfaces. Environ. Microbiol. 20, 958–970. https://doi.org/10.1111/1462-2920.14024.

Burgos-Cara, A., Ruiz-Agudo, E., Rodriguez-Navarro, C., 2017. Effectiveness of oxalic acid treatments for the protection of marble surfaces. Mater. Des. 115, 82–92. https://doi.org/10.1016/j.matdes.2016.11.037.

Buss, H.L., Lüttge, A., Brantley, S.L., 2007. Etch pit formation on iron silicate surfaces during siderophore-promoted dissolution. Chem. Geol. 240, 326–342. https://doi.org/10.1016/j.chemgeo.2007.03.003.

Callahan, B.J., McMurdie, P.J., Rosen, M.J., Han, A.W., Johnson, A.J.A., Holmes, S.P., 2016. DADA2: high-resolution sample inference from Illumina amplicon data. Nat. Methods 13, 581–583. https://doi.org/10.1038/nmeth.3869.

Cámara, B., de los Ríos, A., del Cura, M.A.G., Galván, V., Ascaso, C., 2008. Dolostone bioreceptivity to fungal colonization. Mater. Constr. 58, 113–124. https://doi.org/10.3989/mc.2008.v58.i289-290.71.

Cañaveras, J.C., Sanz-Rubio, E., Sánchez-Moral, S., 2022. Weathering processes on sandstone painting and carving surfaces at prehistoric rock sites in southern Spain. Appl. Sci. 12, 5330. https://doi.org/10.3390/app12115330.

Chazdon, R.L., Chao, A., Colwell, R.K., Lin, S.-Y., Norden, N., Letcher, S.G., Clark, D.B., Finegan, B., Arroyo, J.P., 2011. A novel statistical method for classifying habitat generalists and specialists. Ecology 92, 1332–1343. https://doi.org/10.1890/10-1345.1.

Chen, J., Li, F., Zhao, X., Wang, Y., Zhang, L., Yan, L., Yu, L., 2022. Change in composition and potential functional genes of microbial communities on carbonatite rinds with different weathering times. Front. Microbiol. 13, 1024672. https://doi.org/10.3389/fmicb.2022.1024672.

Cheng, Y., Hubbard, C.G., Zheng, L., Arora, B., Li, L., Karaoz, U., Ajo-Franklin, J., Bouskill, N.J., 2018. Next generation modeling of microbial souring – parameterization through genomic information. Int. Biodeterior. Biodegradation 126, 189–203. https://doi.org/10.1016/j.ibiod.2017.06.014.

Clark, J.D., 1945. Short notes on stone age sites at Yavelo, Southern Abyssinia. R. Soc. South Africa 31, 29–37.

Coppock, D.L., 1994. The Borana Plateau of Southern Ethiopia: Synthesis of Pastoral Research, Development and Change, 1980–91 (Report). International Livestock Centre for Africa.

Cordero, P.R.F., Bayly, K., Man Leung, P., Huang, C., Islam, Z.F., Schittenhelm, R.B., King, G.M., Greening, C., 2019. Atmospheric carbon monoxide oxidation is a widespread mechanism supporting microbial survival. ISME J. 13, 2868–2881. https://doi.org/10.1038/s41396-019-0479-8.

Das, M., Ghosh, T.S., Jeffery, I.B., 2020. IPCO: inference of pathways from co-variance analysis. BMC Bioinformatics 21, 62. https://doi.org/10.1186/s12859-020-3404-2.

Ding, X., Lan, W., Li, Y., Yan, A., Katayama, Y., Koba, K., Makabe, A., Fukushima, K., Yano, M., Onishi, Y., Ge, Q., Gu, J.-D., 2021. An internal recycling mechanism between ammonia/ammonium and nitrate driven by ammonia-oxidizing archaea and bacteria (AOA, AOB, and Comammox) and DNRA on Angkor sandstone monuments. Int. Biodeterior. Biodegradation 165, 105328. https://doi.org/10.1016/j.ibiod.2021.105328.

Ding, X., Lan, W., Yan, A., Li, Y., Katayama, Y., Gu, J.-D., 2022. Microbiome characteristics and the key biochemical reactions identified on stone world cultural heritage under different climate conditions. J. Environ. Manag. 302, 114041 https://doi.org/10.1016/j.jenvman.2021.114041.

Dini-Andreote, F., Stegen, J.C., van Elsas, J.D., Salles, J.F., 2015. Disentangling mechanisms that mediate the balance between stochastic and deterministic processes in microbial succession. Proc. Natl. Acad. Sci. 112, E1326–E1332. https://doi.org/10.1073/pnas.1414261112.

Dorn, (last) R.I., 1998. Rock coatings. In: Developments in Earth Surface Processes 6. Elsevier, Amsterdam.

Douglas, G.M., Maffei, V.J., Zaneveld, J.R., Yurgel, S.N., Brown, J.R., Taylor, C.M., Huttenhower, C., Langille, M.G.I., 2020. PICRUSt2 for prediction of metagenome functions. Nat. Biotechnol. 38, 685–688. https://doi.org/10.1038/s41587-020-0548-6.

Farhat, M.B., Boukhris, I., Chouayekh, H., 2015. Mineral phosphate solubilization by Streptomyces sp. CTM396 involves the excretion of gluconic acid and is stimulated by humic acids. FEMS Microbiol. Lett. 362, fnv008. https://doi.org/10.1093/femsle/fnv008.

Favero-Longo, S.E., Viles, H.A., 2020. A review of the nature, role and control of lithobionts on stone cultural heritage: weighing-up and managing biodeterioration and bioprotection. World J. Microbiol. Biotechnol. 36, 100. https://doi.org/10.1007/s11274-020-02878-3.

Ferrier, J., Csetenyi, L., Gadd, G.M., 2022. Fungal transformation of natural and synthetic cobalt-bearing manganese oxides and implications for cobalt biogeochemistry. Environ. Microbiol. 24, 667–677. https://doi.org/10.1111/1462-2920.15526.

Fierer, N., Bradford, M.A., Jackson, R.B., 2007. Toward an ecological classification of soil bacteria. Ecology 88, 1354–1364. https://doi.org/10.1890/05-1839.

Filippidou, S., Wunderlin, T., Junier, T., Jeanneret, N., Dorador, C., Molina, V., Johnson, D.R., Junier, P., 2016. A combination of extreme environmental conditions favor the prevalence of endospore-forming Firmicutes. Front. Microbiol. 7.

Friedrich, C.G., Rother, D., Bardischewsky, F., Quentmeier, A., Fischer, J., 2001. Oxidation of reduced inorganic sulfur compounds by Bacteria: emergence of a common mechanism? Appl. Environ. Microbiol. 67, 2873–2882. https://doi.org/10.1128/AEM.67.7.2873-2882.2001.

Gadd, G.M., Rhee, Y.J., Stephenson, K., Wei, Z., 2012. Geomycology: metals, actinides and biominerals. Environ. Microbiol. Rep. 4, 270–296. https://doi.org/10.1111/j.1758-2229.2011.00283.x.

Gadd, G.M., Bahri-Esfahani, J., Li, Q., Rhee, Y.J., Wei, Z., Fomina, M., Liang, X., 2014. Oxalate production by fungi: significance in geomycology, biodeterioration and bioremediation. Fungal Biol. Rev. 28, 36–55. https://doi.org/10.1016/j.fbr.2014.05.001.

Gallinaro, M., Zerboni, A., 2021a. Rock, pigments, and weathering. A preliminary assessment of the challenges and potential of physical and biochemical studies on rock art from southern Ethiopia. Quaternary International, Impacts of scientific approaches on Rock Art research: global perspectives 572, 41–51. https://doi.org/10.1016/j.quaint.2020.05.056.

Gallinaro, M., Zerboni, A., 2021b. Rock, pigments, and weathering. A preliminary assessment of the challenges and potential of physical and biochemical studies on rock art from southern Ethiopia. Quat. Int. 572, 41–51. https://doi.org/10.1016/j.quaint.2020.05.056.

Gallinaro, M., Zerboni, A., Solomon, T., Spinapolice, E.E., 2018. Rock art between preservation, research and sustainable development—a perspective from southern Ethiopia. Afr. Archaeol. Rev. 35, 211–223.

Gambino, M., Lepri, G., Štovícek, A., Ghazayarn, L., Villa, F., Gillor, O., Cappitelli, F., 2021. The tombstones at the Monumental Cemetery of Milano select for a specialized microbial community. Int. Biodeterior. Biodegrad. 164 https://doi.org/10.1016/j.ibiod.2021.105298.

Gonzalez, I., Laiz, L., Hermosin, B., Caballero, B., Incerti, C., Saiz-Jimenez, C., 1999. Bacteria isolated from rock art paintings: the case of Atlanterra shelter (South Spain). J. Microbiol. Methods 36, 123–127. https://doi.org/10.1016/s0167-7012(99)00017-2.

González-Gómez, W.S., Quintana, P., Gómez-Cornelio, S., García-Solis, C., Sierra-Fernandez, A., Ortega-Morales, O., De la Rosa-García, S.C., 2018. Calcium oxalates in biofilms on limestone walls of Maya buildings in Chichén Itzá. Mexico. Environ. Earth Sci. 77, 230. https://doi.org/10.1007/s12665-018-7406-6.

Green, H., Gleadow, A., Levchenko, V.A., Finch, D., Myers, C., McGovern, J., Heaney, P., Pickering, R., 2021. Dating correlated microlayers in oxalate accretions from rock art shelters: new archives of paleoenvironments and human activity. Sci. Adv. 7, eabf3632. https://doi.org/10.1126/sciadv.abf3632.

Greening, C., Grinter, R., 2022. Microbial oxidation of atmospheric trace gases. Nat. Rev. Microbiol. 20, 513–528. https://doi.org/10.1038/s41579-022-00724-x.

Greening, C., Carere, C.R., Rushton-Green, R., Harold, L.K., Hards, K., Taylor, M.C., Morales, S.E., Stott, M.B., Cook, G.M., 2015. Persistence of the dominant soil phylum Acidobacteria by trace gas scavenging. Proc. Natl. Acad. Sci. 112, 10497–10502. https://doi.org/10.1073/pnas.1508385112.

He, J., Zhang, N., Shen, X., Muhammad, A., Shao, Y., 2022. Deciphering environmental resistome and mobilome risks on the stone monument: a reservoir of antimicrobial resistance genes. Sci. Total Environ. 838, 156443 https://doi.org/10.1016/j.scitotenv.2022.156443.

Hernanz, A., Gavira-Vallejo, J.M., Ruiz-López, J., 2007. Calcium oxalates and prehistoric paintings. The usefulness of these biomaterials. J. Optoelectron. Adv. 9, 512–521.

Huntley, J., Aubert, M., Oktaviana, A.A., Lebe, R., Hakim, B., Burhan, B., Aksa, L.M., Geria, I.M., Ramli, M., Siagian, L., Brand, H.E.A., Brumm, A., 2021. The effects of climate change on the Pleistocene rock art of Sulawesi. Sci. Rep. 11, 9833. https://doi.org/10.1038/s41598-021-87923-3.

Imhoff, J.F., Rahn, T., Künzel, S., Neulinger, S.C., 2018. Photosynthesis is widely distributed among Proteobacteria as demonstrated by the phylogeny of PufLM reaction center proteins. Front. Microbiol. 8, 318180 https://doi.org/10.3389/fmicb.2017.02679.

Imhoff, J.F., Rahn, T., Künzel, S., Neulinger, S.C., 2019. Phylogeny of Anoxygenic photosynthesis based on sequences of photosynthetic reaction center proteins and a key enzyme in bacteriochlorophyll biosynthesis, the Chlorophyllide reductase. Microorganisms 7, 576. https://doi.org/10.3390/microorganisms7110576.

Islam, Z.F., Cordero, P.R.F., Feng, J., Chen, Y.-J., Bay, S.K., Jirapanjawat, T., Gleadow, R. M., Carere, C.R., Stott, M.B., Chiri, E., Greening, C., 2019. Two Chloroflexi classes independently evolved the ability to persist on atmospheric hydrogen and carbon monoxide. ISME J. 13, 1801–1813. https://doi.org/10.1038/s41396-019-0393-0.

Jeong, S.-W., Jung, J.-H., Kim, M.-K., Seo, H.S., Lim, H.-M., Lim, S., 2016. The three catalases in Deinococcus radiodurans: only two show catalase activity. Biochem. Biophys. Res. Commun. 469, 443–448. https://doi.org/10.1016/j.bbrc.2015.12.017.

Ji, M., Greening, C., Vanwonterghem, I., Carere, C.R., Bay, S.K., Steen, J.A., Montgomery, K., Lines, T., Beardall, J., van Dorst, J., Snape, I., Stott, M.B., Hugenholtz, P., Ferrari, B.C., 2017. Atmospheric trace gases support primary production in Antarctic desert surface soil. Nature 552, 400–403. https://doi.org/10.1038/nature25014.

Jin, M., Xiao, A., Zhu, L., Zhang, Z., Huang, H., Jiang, L., 2019. The diversity and commonalities of the radiation-resistance mechanisms of Deinococcus and its up-to-date applications. AMB Express 9, 138. https://doi.org/10.1186/s13568-019-0862-x.

King, G.M., 2003. Molecular and culture-based analyses of aerobic carbon monoxide oxidizer diversity. Appl. Environ. Microbiol. 69, 7257–7265. https://doi.org/10.1128/AEM.69.12.7257-7265.2003.

King, G.M., Weber, C.F., 2007. Distribution, diversity and ecology of aerobic CO-oxidizing bacteria. Nat. Rev. Microbiol. 5, 107–118. https://doi.org/10.1038/nrmicro1595.

Kusumi, A., Li, X.S., Katayama, Y., 2011. Mycobacteria isolated from Angkor monument sandstones grow Chemolithoautotrophically by oxidizing elemental sulfur. Front. Microbiol. 2.

Langille, M.G.I., 2018. Exploring linkages between taxonomic and functional profiles of the human microbiome. mSystems 3. https://doi.org/10.1128/msystems.00163-17.

Lee, K.C., Archer, S.D.J., Boyle, R.H., Lacap-Bugler, D.C., Belnap, J., Pointing, S.B., 2016. Niche filtering of Bacteria in soil and rock habitats of the Colorado Plateau Desert, Utah, USA. Front. Microbiol. 7, 1489. https://doi.org/10.3389/fmicb.2016.01489.

Li, Q., Zhang, B., Yang, X., Ge, Q., 2018. Deterioration-associated microbiome of stone monuments: structure, variation, and assembly. Appl. Environ. Microbiol. 84 https://doi.org/10.1128/AEM.02680-17 e02680-17.

Li, X., Arai, H., Shimoda, I., Kuraishi, H., Katayama, Y., 2008. Enumeration of sulfur-oxidizing microorganisms on deteriorating stone of the Angkor Monuments, Cambodia. Microbes and environments/JSME 23, 293–298. https://doi.org/10.1264/jsme2.ME08521.

Liang, J.-L., Liu, J., Jia, P., Yang, T., Zeng, Q., Zhang, S., Liao, B., Shu, W., Li, J., 2020. Novel phosphate-solubilizing bacteria enhance soil phosphorus cycling following

ecological restoration of land degraded by mining. ISME J. 14, 1600–1613. https://doi.org/10.1038/s41396-020-0632-4.
Liu, X., Koestler, R.J., Warscheid, T., Katayama, Y., Gu, J.-D., 2020. Microbial deterioration and sustainable conservation of stone monuments and buildings. Nat. Sustain. 3, 991–1004. https://doi.org/10.1038/s41893-020-00602-5.
Liu, X., Qian, Y., Wu, F., Wang, Y., Wang, W., Gu, J.-D., 2022. Biofilms on stone monuments: biodeterioration or bioprotection? Trends Microbiol. 30, 816–819. https://doi.org/10.1016/j.tim.2022.05.012.
Luo, G., Xue, C., Jiang, Q., Xiao, Y., Zhang, F., Guo, S., Shen, Q., Ling, N., 2020. Soil carbon, nitrogen, and phosphorus cycling microbial populations and their resistance to global change depend on soil C:N:P stoichiometry. mSystems 5, e00162-20. https://doi.org/10.1128/mSystems.00162-20.
Macholdt, D.S., Jochum, K.P., Al-Amri, A., Andreae, M.O., 2019. Rock varnish on petroglyphs from the Hima region, southwestern Saudi Arabia: chemical composition, growth rates, and tentative ages. The Holocene 29, 1377–1395. https://doi.org/10.1177/0959683619846979.
Meslier, V., Casero, M.C., Dailey, M., Wierzchos, J., Ascaso, C., Artieda, O., McCullough, P.R., DiRuggiero, J., 2018. Fundamental drivers for endolithic microbial community assemblies in the hyperarid Atacama Desert. Environ. Microbiol. 20, 1765–1781. https://doi.org/10.1111/1462-2920.14106.
Mohammadipanah, F., Wink, J., 2016. Actinobacteria from arid and desert habitats: diversity and biological activity. Front. Microbiol. 6, 1541. https://doi.org/10.3389/fmicb.2015.01541.
Murray, B., Ertekin, E., Dailey, M., Soulier, N.T., Shen, G., Bryant, D.A., Perez-Fernandez, C., DiRuggiero, J., 2022. Adaptation of Cyanobacteria to the endolithic light spectrum in hyper-arid deserts. Microorganisms 10, 1198. https://doi.org/10.3390/microorganisms10061198.
Nir, I., Barak, H., Kramarsky-Winter, E., Kushmaro, A., 2019a. Seasonal diversity of the bacterial communities associated with petroglyphs sites from the Negev Desert, Israel. Ann. Microbiol. 69, 1079–1086. https://doi.org/10.1007/s13213-019-01509-z.
Nir, I., Barak, Hana, Baruch, Yifat, Kramarsky-Winter, Esti, Kushmaro, Ariel, 2019b. Insights into bacterial communities associated with petroglyph sites from the Negev Desert, Israel. J. Arid Environ. 166, 79–82. https://doi.org/10.1016/j.jaridenv.2019.04.010.
Nir, I., Barak, H., Kramarsky-Winter, E., Kushmaro, A., de los Ríos, A., 2022. Microscopic and biomolecular complementary approaches to characterize bioweathering processes at petroglyph sites from the Negev Desert, Israel. Environ. Microbiol. 24, 967–980. https://doi.org/10.1111/1462-2920.15635.
Northup, D.E., Snider, J.R., Spilde, M.N., Porter, M.L., van de Kamp, J.L., Boston, P.J., Nyberg, A.M., Bargar, J.R., 2010. Diversity of rock varnish bacterial communities from Black Canyon, New Mexico. J. Geophys. Res. Biogeo. 115 https://doi.org/10.1029/2009JG001107.
Patrauchan, M.A., Miyazawa, D., LeBlanc, J.C., Aiga, C., Florizone, C., Dosanjh, M., Davies, J., Eltis, L.D., Mohn, W.W., 2012. Proteomic analysis of survival of Rhodococcus jostii RHA1 during carbon starvation. Appl. Environ. Microbiol. 78, 6714–6725. https://doi.org/10.1128/AEM.01293-12.
Pedrinho, A., Mendes, L.W., Merloti, L.F., Andreote, F.D., Tsai, S.M., 2020. The natural recovery of soil microbial community and nitrogen functions after pasture abandonment in the Amazon region. FEMS Microbiol. Ecol. 96, fiaa149. https://doi.org/10.1093/femsec/fiaa149.
Perez, A., Rossano, S., Trcera, N., Huguenot, D., Fourdrin, C., Verney-Carron, A., van Hullebusch, E.D., Guyot, F., 2016. Bioalteration of synthetic Fe(III)-, Fe(II)-bearing basaltic glasses and Fe-free glass in the presence of the heterotrophic bacteria strain Pseudomonas aeruginosa: impact of siderophores. Geochim. Cosmochim. Acta 188, 147–162. https://doi.org/10.1016/j.gca.2016.05.028.
Pinna, D., 2014. Biofilms and lichens on stone monuments: do they damage or protect? Front. Microbiol. 5, 133. https://doi.org/10.3389/fmicb.2014.00133.
Portillo, M.C., Saiz-Jimenez, C., Gonzalez, J.M., 2009. Molecular characterization of total and metabolically active bacterial communities of "white colonizations" in the Altamira cave, Spain. Res. Microbiol. 160, 41–47. https://doi.org/10.1016/j.resmic.2008.10.002.
Potysz, A., Bartz, W., 2022. Bioweathering of minerals and dissolution assessment by experimental simulations—implications for sandstone rocks: a review. Constr. Build. Mater. 316, 125862 https://doi.org/10.1016/j.conbuildmat.2021.125862.
Qian, Y., Gan, T., Zada, S., Katayama, Y., Gu, J.-D., 2022. De-calcification as an important mechanism in (bio)deterioration of sandstone of Angkor monuments in Cambodia. Int. Biodeterior. Biodegradation 174, 105470. https://doi.org/10.1016/j.ibiod.2022.105470.
Qian, Z., Tianwei, H., Mackey, H.R., van Loosdrecht, M.C.M., Guanghao, C., 2019. Recent advances in dissimilatory sulfate reduction: from metabolic study to application. Water Res. 150, 162–181. https://doi.org/10.1016/j.watres.2018.11.018.
Quast, C., Pruesse, E., Yilmaz, P., Gerken, J., Schweer, T., Yarza, P., Peplies, J., Glöckner, F.O., 2013. The SILVA ribosomal RNA gene database project: improved data processing and web-based tools. Nucleic Acids Res. 41, D590–D596. https://doi.org/10.1093/nar/gks1219.
R Core Team, 2021. R: A Language and Environment for Statistical Computing. R Foundation for Statistical Computing, Vienna, Austria. URL. https://www.R-project.org/.
Rabbachin, L., Piñar, G., Nir, I., Kushmaro, A., Pavan, M.J., Eitenberger, E., Waldherr, M., Graf, A., Sterflinger, K., 2022. A multi-analytical approach to infer mineral–microbial interactions applied to petroglyph sites in the negev desert of israel. Appl. Sci. 12, 6936. https://doi.org/10.3390/app12146936.
Rapin, A., Pattaroni, C., Marsland, B.J., Harris, N.L., 2017. Microbiota analysis using an Illumina MiSeq platform to sequence 16S rRNA genes. Curr. Protoc. Mouse Biol. 7, 100–129. https://doi.org/10.1002/cpmo.29.
Ray, A.E., Zaugg, J., Benaud, N., Chelliah, D.S., Bay, S., Wong, H.L., Leung, P.M., Ji, M., Terauds, A., Montgomery, K., Greening, C., Cowan, D.A., Kong, W., Williams, T.J., Hugenholtz, P., Ferrari, B.C., 2022. Atmospheric chemosynthesis is phylogenetically and geographically widespread and contributes significantly to carbon fixation throughout cold deserts. ISME J. 16, 2547–2560. https://doi.org/10.1038/s41396-022-01298-5.
Ren, Z., Gao, H., Elser, J.J., Zhao, Q., 2017. Microbial functional genes elucidate environmental drivers of biofilm metabolism in glacier-fed streams. Sci. Rep. 7, 12668. https://doi.org/10.1038/s41598-017-13086-9.
Roldán, C., Murcia-Mascarós, S., López-Montalvo, E., Vilanova, C., Porcar, M., 2018. Proteomic and metagenomic insights into prehistoric Spanish Levantine Rock Art. Sci. Rep. 8, 10011. https://doi.org/10.1038/s41598-018-28121-6.
Rolli, E., Marasco, R., Fusi, M., Scaglia, B., Schubotz, F., Mapelli, F., Ciccazzo, S., Brusetti, L., Trombino, L., Tambone, F., Adani, F., Borin, S., Daffonchio, D., 2022. Environmental micro-niche filtering shapes bacterial pioneer communities during primary colonization of a Himalayas' glacier forefield. Environ. Microbiol. 24, 5998–6016. https://doi.org/10.1111/1462-2920.16268.
Saadouli, I., Marasco, R., Mejri, L., Hamden, H., Guerfali, M.M., Stathopoulou, P., Daffonchio, D., Cherif, A., Ouzari, H.-I., Tsiamis, G., Mosbah, A., 2022. Diversity and adaptation properties of actinobacteria associated with Tunisian stone ruins. Front. Microbiol. 13.
Sazanova, K.V., Zelenskaya, M.S., Vlasov, A.D., Bobir, S.Yu., Yakkonen, K.L., Vlasov, D. Yu., 2022. Microorganisms in superficial deposits on the stone monuments in Saint Petersburg. Microorganisms 10, 316. https://doi.org/10.3390/microorganisms10020316.
Schabereiter-Gurtner, C., Saiz-Jimenez, C., Piñar, G., Lubitz, W., Rölleke, S., 2004. Phylogenetic diversity of bacteria associated with Paleolithic paintings and surrounding rock walls in two Spanish caves (Llonín and La Garma). FEMS Microbiol. Ecol. 47, 235–247. https://doi.org/10.1016/S0168-6496(03)00280-0.
Schellhorn, H.E., 2020. Function, evolution, and composition of the RpoS regulon in Escherichia coli. Front. Microbiol. 11.
Smith, T.P., Mombrikotb, S., Ransome, E., Kontopoulos, D.-G., Pawar, S., Bell, T., 2022. Latent functional diversity may accelerate microbial community responses to temperature fluctuations. eLife 11, e80867. https://doi.org/10.7554/eLife.80867.
Speirs, L.B.M., Rice, D.T.F., Petrovski, S., Seviour, R.J., 2019. The phylogeny, biodiversity, and ecology of the Chloroflexi in activated sludge. Front. Microbiol. 10.
Sun, Y., Wang, C., Yang, J., Liao, J., Chen, H.Y.H., Ruan, H., 2021. Elevated CO2 shifts soil microbial communities from K- to r-strategists. Glob. Ecol. Biogeogr. 30, 961–972. https://doi.org/10.1111/geb.13281.
Sutter, P., n.d. CARE Borena Rangelands Development Project. Socio-Economic Baseline Study. CARE International in Ethiopia Unpublished Report. Addis Ababa. 1995.
Syed, S., Buddolla, V., Lian, B., 2020. Oxalate carbonate pathway—conversion and fixation of soil carbon—a potential scenario for sustainability. Front. Plant Sci. 11.
Tian, J., Ge, F., Zhang, D., Deng, S., Liu, X., 2021. Roles of phosphate solubilizing microorganisms from managing soil phosphorus deficiency to mediating biogeochemical P cycle. Biology (Basel) 10, 158. https://doi.org/10.3390/biology10020158.
Torres, M.A., West, A.J., Nealson, K., 2014. Microbial Acceleration of Olivine Dissolution via Siderophore Production. Procedia Earth and Planetary Science, Geochemistry of the Earth's surface GES-10 Paris France, 18–23 August, 2014, 10, pp. 118–122. https://doi.org/10.1016/j.proeps.2014.08.041.
Vadstein, O., Attramadal, K.J.K., Bakke, I., Olsen, Y., 2018. K-selection as microbial community management strategy: a method for improved viability of larvae in aquaculture. Front. Microbiol. 9.
Varliero, G., Anesio, A.M., Barker, G.L.A., 2021. A taxon-wise insight into rock weathering and nitrogen fixation functional profiles of proglacial systems. Front. Microbiol. 12.
Villa, F., Cappitelli, F., 2019. The ecology of subaerial biofilms in dry and inhospitable terrestrial environments. Microorganisms 7, 380. https://doi.org/10.3390/microorganisms7100380.
Villa, F., Stewart, P.S., Klapper, I., Jacob, J.M., Cappitelli, F., 2016. Subaerial biofilms on outdoor stone monuments: changing the perspective toward an ecological framework. BioScience 66, 285–294. https://doi.org/10.1093/biosci/biw006.
Villa, F., Gulotta, D., Toniolo, L., Borruso, L., Cattò, C., Cappitelli, F., 2020. Aesthetic alteration of marble surfaces caused by biofilm formation: effects of chemical cleaning. Coatings 10, 122. https://doi.org/10.3390/coatings10020122.
Walters, K.E., Martiny, J.B.H., 2020. Alpha-, beta-, and gamma-diversity of bacteria varies across habitats. PLoS One 15, e0233872. https://doi.org/10.1371/journal.pone.0233872.
Wang, Y., Zhao, R., Liu, L., Li, B., Zhang, T., 2021. Selective enrichment of comammox from activated sludge using antibiotics. Water Res. 197, 117087 https://doi.org/10.1016/j.watres.2021.117087.
Wei, Z., Hillier, S., Gadd, G.M., 2012. Biotransformation of manganese oxides by fungi: solubilization and production of manganese oxalate biominerals. Environ. Microbiol. 14, 1744–1753. https://doi.org/10.1111/j.1462-2920.2012.02776.x.
Wild, B., Gerrits, R., Bonneville, S., 2022. The contribution of living organisms to rock weathering in the critical zone. NPJ Mater. Degrad. 6, 1–16. https://doi.org/10.1038/s41529-022-00312-7.
Wu, Y.-L., Villa, F., Mugnai, G., Gallinaro, M., Spinapolice, E.E., Zerboni, A., 2020. Geomicrobial investigations of colored outer coatings from an Ethiopian rock art gallery. Coatings 10, 536. https://doi.org/10.3390/coatings10060536.

Yadav, P., Singh, R.P., Rana, S., Joshi, D., Kumar, D., Bhardwaj, N., Gupta, R.K., Kumar, A., 2022. Mechanisms of stress tolerance in Cyanobacteria under extreme conditions. Stresses 2, 531–549. https://doi.org/10.3390/stresses2040036.

Yin, Q., Sun, Y., Li, B., Feng, Z., Wu, G., 2022. The r/K selection theory and its application in biological wastewater treatment processes. Sci. Total Environ. 824, 153836 https://doi.org/10.1016/j.scitotenv.2022.153836.

Zanardini, E., May, E., Purdy, K.J., Murrell, J.C., 2019. Nutrient cycling potential within microbial communities on culturally important stoneworks. Environ. Microbiol. Rep. 11, 147–154. https://doi.org/10.1111/1758-2229.12707.

Zerboni, A., 2008. Holocene rock varnish on the Messak plateau (Libyan Sahara): chronology of weathering processes. Geomorphology 102, 640–651. https://doi.org/10.1016/j.geomorph.2008.06.010.

Zerboni, A., Villa, F., Wu, Y.-L., Solomon, T., Trentini, A., Rizzi, A., Cappitelli, F., Gallinaro, M., 2022. The sustainability of rock art: preservation and research. Sustainability 14, 6305. https://doi.org/10.3390/su14106305.

Zhang, G., Gong, C., Gu, J., Katayama, Y., Someya, T., Gu, J.-D., 2019. Biochemical reactions and mechanisms involved in the biodeterioration of stone world cultural heritage under the tropical climate conditions. Int. Biodeterior. Biodegradation 143, 104723. https://doi.org/10.1016/j.ibiod.2019.104723.

Zhang, X., Liu, S., Wang, J., Huang, Y., Freedman, Z., Fu, S., Liu, K., Wang, H., Li, X., Yao, M., Liu, X., Schuler, J., 2020. Local community assembly mechanisms shape soil bacterial β diversity patterns along a latitudinal gradient. Nat. Commun. 11, 5428. https://doi.org/10.1038/s41467-020-19228-4.